APPLICATION OF COIR GEOTEXTILES IN RURAL ROADS OF INDIA

G. Venkatappa Rao[1], Evangeline Y. Sheela[2] and M. K. Sayida[3]

ABSTRACT

Worldwide, there is continuous search for finding new materials for use in civil/geotechnical Engineering practice. This paper presents the emergence of one such material known as coir geotextiles. Efforts have been made to present the significant technological developments that have taken place in the evolution of coir geotextiles, particularly for application in low-volume roads. This paper summarizes the various studies conducted to evaluate the potential of coir geotextiles through extensive laboratory model studies and field trials.

***Keywords** : Coir geotextiles Reinforcement Rural roads*

RURAL ROADS

The rural roads in India form a substantial portion of the Indian road network. About 600 million people live in nearly 0.6 million villages scattered over the country. Rural roads provide the means to bring the rural population to main stream. They comprise village roads (VRs) and other district roads (ODRs) and are normally under the jurisdiction of the Public Works Departments or Rural Development Departments within the state government administration.

Pradhan Mantri Gram Sadak Yojana (PMGSY) was launched by the Government of India in December 2000 to provide all weather rural road connectivity to every rural habitation with a minimum population of 500 in the plains and 250-plus in hill states, tribal districts and desert areas. This programme has so far covered 178,184 habitations as per the criteria laid down. Out of them, 64% of these habitations have road today. Since its inception, it has provided connectivity of over 4.66 Lakh km including upgradation of 1.67 Lakh km of existing roads.

This scheme is one of the most successful initiatives in rural India. By March 2019, all states and UTs are expected to complete PMGSY-I by connecting all eligible habitations with 500 and 250 populations as per 2001 Census. Some states have not only completed connectivity for eligible habitations but have also completed Phase-II of PMGSY which took up 25 percent of district rural roads for upgradation. It is now proposed that states completing Phase-I and Phase-II successfully could be taken up in the proposed PMGSY-III for connecting upgrading all 250 plus habitations as per 2011 Census. The target of PMGSY-III is to construct/upgrade 120,000 km of roads to benefit about 40,000 habitations.

Rural road connectivity remains a highly important priority, and as a result similar programmes are ongoing in many states to connect smaller communities.

GEOSYNTHETICS IN RURAL ROADS

For the construction of rural roads, Indian Road Congress has bought out Rural Road Manual IRC SP: 20-2002/2010 for design and construction.

The design is based on the CBR value of the soil subgrade and the 10-year projected cumulative traffic with an assumed 6% traffic growth per year. Based on this concept, normally two layers of WBM with 75 mm thickness is laid over the granular subbase with suitable material having minimum CBR of 15. However, there are situations in many states where the prescribed standards are not available at normal leads resulting in longer haulage and higher costs. Several types of new materials are tried to reduce the cost of construction. One such a material is coir geotextile, a common natural fibre type of geosynthetic. The main function of geosynthetics in the unpaved rural road is separation, the secondary functions being reinforcement and filtration/drainage. Placing an appropriate geotextile between the granular subbase and soft subgrade helps to stabilize an unpaved road in a number of ways as in Fig. 1.

Site conditions which benefit from geotextile stabilization include:

1 Department of Civil Engineering, Indian Institute of Technology Gandhinagar, Gandhinagar
2 Department of Civil Engineering, Mohandas College of Engineering and Technology, Nedumangad, Thiruvananthapuram
3 Department of Civil Engineering, College of Engineering Trivandrum, Thiruvananthapuram

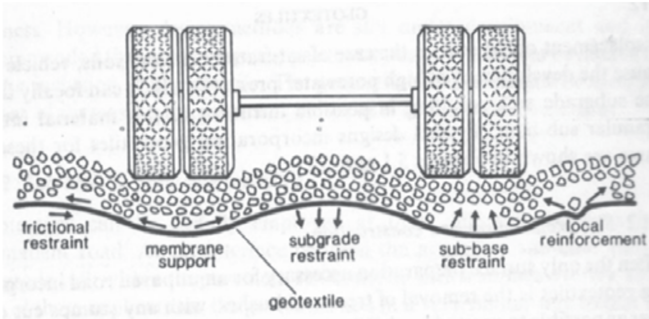

Fig. 1 : Geotextile stabilization of an unpaved road

- Poor soils (i.e. USCS classification SC, CL, CH, ML, OL, OH, and Pt.)
- Soils with low undrained shear strength, c\100 kPa
- Water table near ground surface.
- Seasonally wet subgrade conditions.
- High-sensitivity soils

GENESIS

'CocosNucifera' the fibre which surrounds the bare shell of a coconut protecting the kernel provides the material for coir industry. Depending on the process of extracting the fibres from the husks, coir is classified into two varieties, namely, 'white coir' and 'brown coir'. In India, white coir is produced from husks of mature green coconuts by subjecting the husk to a retting process of 1 to 3 months, followed by manual separation of fibre from the pith surrounding it. On the other hand, brown coir is produced from dry/semi-dry coconut husks by a mechanical process. White coir is utilized from production of more durable, value added goods (like carpets etc.), whereas brown coir which is inexpensive is used in the manufacturing of geotextiles. Coir industry in India in the southern region is well developed, the overall production being around 2,50,000 tonnes/annum. Recent estimates reveal that India produces nearly 70% of the world production of coir as per FAO statistics. Views of the Coconut husk and coir fibre are shown in Fig. 2. The woven coir geotextiles and the blankets that are being manufactured in India are depicted in Fig. 3a, b.

The high lignin content of coir fibre (to the extent of 37%) differentiates it from all other natural fibres, and as such they have much longer life under various environmental conditions [1]. Typical result of degradation of coir under saturated clay conditions is depicted in Fig. 4, from which it is evident the degradation of brown coir used to manufacture geotextiles is hardly 25% in 6 months.

Extensive work has been carried out at IIT Delhi to characterize coir geotextiles [2, 3] which led to the development of Indian Standards for testing them. The typical properties of woven coir geotextiles are presented in Table 1.

Fig. 2 : A view of the coconut husk and coir fibre

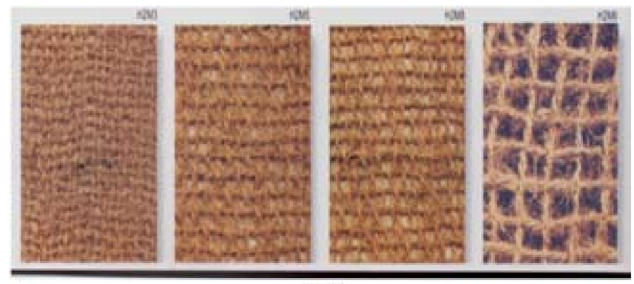

(a)

(b)

Fig. 3 : a Different types of woven coir geotextiles that are manufactured indigenously. b Nonwoven coir geotextile (blanket) manufactured by air-laying and multiple stitching

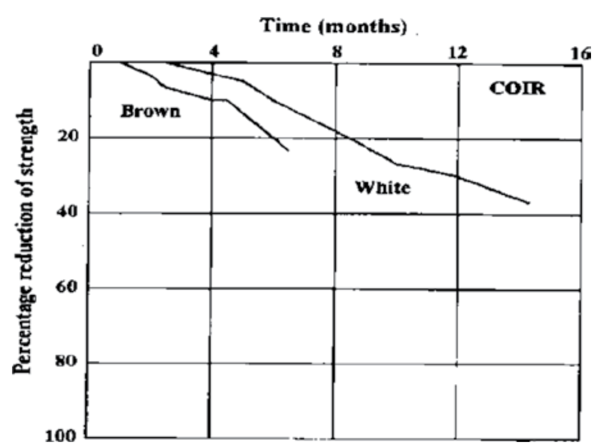

Fig. 4 : Degradation of coir yarn

Table 1 : Typical properties of woven coir geotextiles (after CCRI, Alappuzha)

Sl. No.	Characteristics	Values			Method of test
1	Mass/unit area/g/m²*	400	700	900	IS 15868 (Part 1 to 6)
2	Width in cm, (Min)	100 or as required	100 or as required	100 or as required	IS 12503 (Part 1 to 6)
3	Length in m (Min)	50 or as required	50 or as required	50 or as required	IS 12503 (Part 1 to 6)
4	Thickness at 20 kPa, in mm,*	6.5	6.5	6.5	IS 15868 (Part 1 to 6)
5	Ends (warp)*	180	150	210	IS 12503 (Part 1 to 6)
6	Picks (weft)*	160	160	250	
7	Break load, dry				
	(a) M/D in kN/m	7.0	8.5	15.0	IS 13162 (Part 5)
	(b) CM/D in kN/m	4.0	8.0	8.0	
8	Break load, wet				
	(a) M/D in kN/m	3.0	7.0	12.5	IS 13162 (Part 5)
	(b) CM/D in kN/m*	2.0	4.5	5.0	
9	Peak load, dry				
	(a) M/D in kN/m	7.5	9.0	9.0	IS 13162 (Part 5)
	(b) CM/D in kN/m *	4.0	8.0	18.0	
10	Peak load, wet				
	(a) M/D in kN/m	3.0	8.5	15.0	IS 13162 (Part 5)
	(b) CM/D in kN/m *	2.0	5.5	6.0	
11	Trapezoidal tearing strength at 25 mm gauge length,*				
	(a) M/D in kN/m	0.18	0.35	0.50	
	(b) CM/D in kN/m	0.15	0.30	0.35	
12	Mesh size, mm, **	20.0 9 16.75	7.50 9 7.30	4.2 9 5.1	IS 15868 (Part 1 to 6)

M/D machine direction, CM/D cross machine direction

*Minimum value, ** maximum value

LABORATORY MODEL STUDIES AT IIT DELHI

Coir Geotextiles Used

Monotonic load study with coir geotextiles was conducted by Rao and Dutta [4] by using four different varieties of woven coir geotextiles designated as A, B, C, D and four different varieties of nonwoven coir geotextiles designated as Types E, F, G and H. The woven coir geotextiles Types A, B, C and D are netting composed of 100% coir fibre spun into yarn and woven in conventional flat bed looms in widths of 1, 2 or 4 m. Type E is composed of 100% decurled coir fibreweb of 400 g/m² encased over top and bottom with brown PP netting. The mass per unit area of top and bottom netting is 7.1 g/m² and 4.8 g/m². The matrix is stitched together on 50 mm centres with white PP thread dipped in black natural glue. Type F is similar to Type E except that the coir fibre web is 750 g/m². The nonwoven coir geotextile Type G consists of 100% decurled coir fibre web of 650 g/m² encased over top and bottom with stable woven heavy jute netting. The matrix is stitched together on 50 mm centres with 2-ply jute yarn. The mass per unit area of the top and bottom jute netting is 100 g/m² each. Type H comprises 100% de-curled coir web of 390 g/m² encased over the top with heavy duty woven coir netting of 700 g/m² and at the bottom with brown UV-stabilized PP netting of 4.8 g/m². The matrix is stitched together on 50 mm centres with the heavy 2 ply jute thread. The investigation was carried out on locally available Badarpur sand which is medium-grained uniform quarry sand having subangular particles of weathered quartzite. The sand has a uniformity coefficient of 2.11 and a coefficient of curvature of 0.96. The placement dry unit weight of sand in the test tank was 14.95 kN/m³, and the kaolinite clay is CH.

Test Tank

Model tests were carried out in a tank shown in Fig. 5. The internal dimensions of the tank were 350 mm 9 350 mm in plan and 420 mm in depth. The outer dimensions of this model tank were such that it can be accommodated on the

Hounsfield Universal Testing Machine, a microprocessor controlled universal testing machine of 50 kN static capacity and 25 kN capacity for cyclic loading, with provision for different cross head speeds.

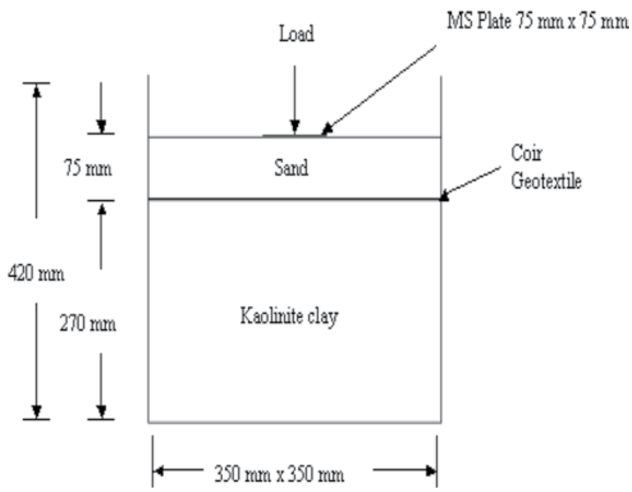

Fig. 5 : Schematic sketch of experimental setup

Test Procedure

At the outset, a thin sheet of polythene was fixed with cello tape over the internal surfaces of the model tank in an attempt to minimize the side friction. At the bottom of the tank, a thin layer of grease was applied. A typical test model consisted of saturated clay subgrade overlain by a sand layer as the base course. Keeping the overall dimensions of the test tank in view, the depth of the subgrade soil in the model tank was kept as 270 mm and the overlying sand was 75 mm thick throughout the study. Kaolinite clay at a moisture content of 36% (previously prepared and kept for 24 h for moisture equilibrium) is placed in the tank by hand-kneading. After the preparation of the subgrade, a geotextile was laid over which a sand course of 75 mm thickness was laid. The normal load was applied centrally through a square steel plate of 75 mm 9 75 mm. The static compression tests were conducted at a deformation rate of 4 mm/min with all the eight coir geotextiles.

In addition, the behaviour of model pavements has also been studied under repeated loading of 17.94 kPa, 35.88 kPa and 71.76 kPa at a test speed of 75 mm/min through 75 mm 9 75 mm square plate. All models were tested up to 1000 repetitions.

Results

The variation of deformation with bearing pressure for all the type of geotextiles is shown in Fig. 6. It is seen that heaviest Type D-reinforced model shows an overall best performance than the other geotextiles A, B and C. At a deformation of 20 mm, whereas the bearing pressure with no geotextile was 54.03 kPa, it increased to 57 kPa for model with Type A woven geotextile, for Type B it was found to be 60.04 kPa, for Type C it was 62.69 kPa and for the heaviest geotextile Type D the value was 75.81 kPa. Consequently, the Types A, B, C and D geotextile-reinforced models exhibited 5%, 11%, 16% and 40% improvement in bearing pressure, which could be attributed to differences in their tensile strength, initial tangent modulus and aperture size. At a deformation of 20 mm, the nonwoven geotextile Type G-reinforced case exhibits an overall best performance than the other nonwovens. The bearing pressures of the unreinforced model being 54.03 kPa improved for the reinforced cases with Types E, F, G, Hf and Hb to 63.71 kPa, 74.01 kPa, 72.58 kPa, 71.84 kPa, 63.13 kPa, respectively. In the same sequence, the reinforced models thus exhibited an improvement of 18%, 37%, 34%, 33% and 17%. It is also interesting to note that the models with nonwovens demonstrated better performance than models of geotextiles reinforced with Types C, B and A. It could be due to the greater direct contact of the nonwoven geotextiles with the soft subgrade, thereby perhaps leading to the better interface friction.

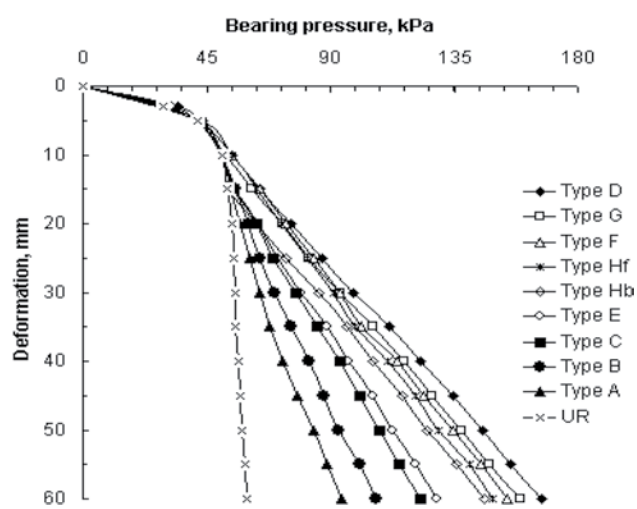

Fig. 6 : Variation of deformation with bearing pressure of all types

Due to the repetitive load, the variation in permanent vertical deformation with a number of load repetitions is reported that the reinforced models consistently performed better than the unreinforced model. The effect is more predominant at large deformations and in general, the increase in permanent deformations decreased with successive load repetitions.

Under a repeated load of 35.88 kPa, the permanent deformation at 200 repetitions was 27.5 mm in the unreinforced model, while in the model reinforced with nonwoven geotextile Type E and woven geotextile Type C the values were 11.30 mm and 12.17 mm, respectively, thereby depicting a significant improvement in the behaviour. Similarly at 700 repetitions, the permanent vertical deformation for the unreinforced model was 63.4 mm, whereas it was only 14.8 mm and 16.1 mm for the model reinforced with Types E and C coir geotextiles as shown in Fig. 7. It may also be observed that up to 50 cycles the behaviour exhibited by both types of geotextiles is nearly the same. But beyond 50 cycles, the nonwoven geotextile Type E performed better than the woven geotextile Type C. This may be due to the direct contact area of nonwoven geotextile offering more interface friction. The improvement is more significant at higher permanent deformation.

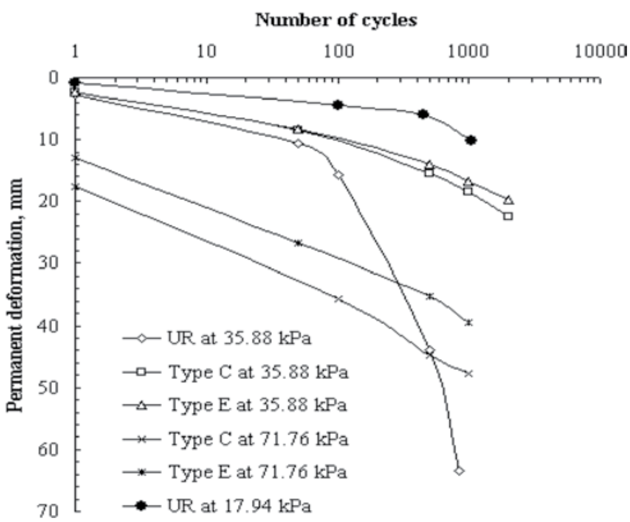

Fig. 7 Permanent vertical deformations versus number of load repetitions behaviour of different models

Fig. 7 : Permanent vertical deformations versus number of load repetitions behaviour of different models

Comparison with Polymeric Woven Geotextile

Based on the research of Sreedhar [5], VenkatappaRao and Sreedhar [5] presented an extensive investigation on the behaviour of coir geotextiles in comparison with a polymeric grid and a geotextile in reference to a pond ash.

Material Characterization

The pond ash was collected from the ash pond of National Thermal Power Corporation (NTPC), Ramagundam plant in Telangana, India. The properties of the pond ash are presented in Table 2.

The woven geotextile (WGT) and the coir geotextile (CGT) used in this study are shown in Figs. 8 and 9.

The primary characteristics of the two geosynthetics used in this study are summarized in Table 3.

The modulus of the geosynthetics was obtained from the wide width tensile strength tests, and the interface friction was obtained from the laboratory pull-out tests.

Table 2 : Engineering characteristics of pond ash

G	1.93
% Gravel	4
% Sand	87
% Silt	3
Plasticity	NP
IS classification	NP
IS heavy compaction test results MDD (kN/cum)	11.7
OMC (%)	29.2
Triaxial UU test results	
At qd = 70% of MDD	0
c (kPa)	31
Φ (deg)	

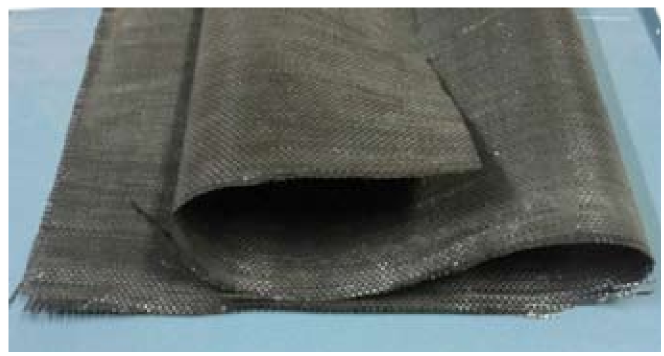

Fig. 8 : A view of the woven geotextile (WGT)

Fig. 9 : A view of the coir geotextile (CGT)

Table 3 : Characteristics of geosynthetics

Product name	Make	Offset modulus (kN/m)	Interface friction factor
Woven geotextile (WGT)	SKAPS W-250	52.17	0.94
Coir woven geotextile (CGT)	CCM, Kerala, India	16.00	1.07

Load Test Facility

A test tank of 750 mm 9 310 mm 9 600 mm (Fig. 10) was fabricated. The pond ash test bed of 250 mm thickness is prepared at 70% of its maximum dry density corresponding to IS heavy compaction test, in five layers of 50 mm thickness each. The pre-test quality was controlled by depth measurements, and the density of the test bed is verified through the pre-placed cups, collected in the post test stage. The load is measured by a load cell of 1 N sensitivity, and the settlement by a LVDT of 0.1 mm sensitivity. The PC controlled test facility allowed feeding the input test conditions, execute, display on line progress, log data at specified interval of 20 s and store it.

Fig. 10 : The test setup for monotonic and cyclic testing

Monotonic Load Tests

In monotonic load tests, the load was applied through a model square footing of 50 mm size (B) with rough base, made of a rigid aluminium plate of 25 mm thickness. The rate of deformation was at 1.25 mm/min. The tests were performed with depth of placement (u) of the reinforcement beneath the base of the footing expressed as (u/B) ratio and application of surcharge expressed in terms of (Df/B) ratio wherein Df is the thickness of the dry sand placed at a density of 16.4 kN/m^3, as shown in Fig. 11.

The basic "bearing pressure versus settlement" plots for pond ash reinforced with WGT and CGT with surcharge are shown in Figs. 12 and 13, respectively.

Cyclic Load Tests

A series of stress-controlled cyclic load tests were performed on the similar reinforced pond ash test beds. The cyclic stress in the range of 0 to 400 kPa was applied at a frequency of 1 Hz, up to 1000 cycles.

The cyclic load test results pertaining to the WGT-reinforced pond ash for different (u/B) ratios in the absence and presence of surcharge are shown in Fig. 14, and those for CGT-reinforced pond ash are shown in Fig. 15.

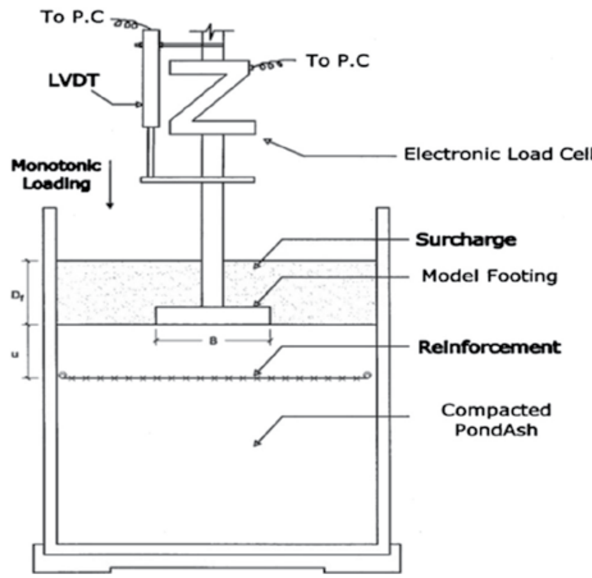

Fig. 11 : Definition sketch of the test procedure

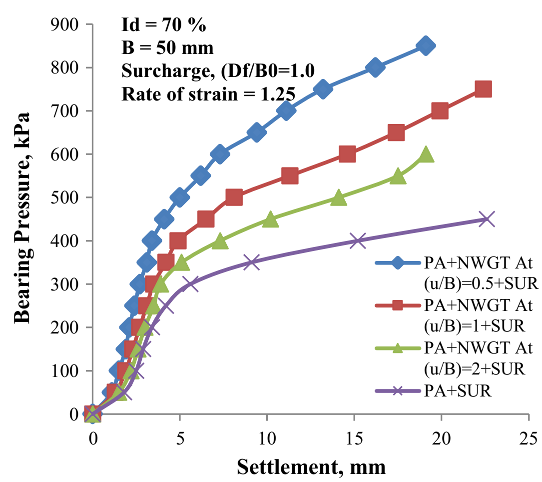

Fig. 12 : Variation of bearing pressure with settlement for WGT

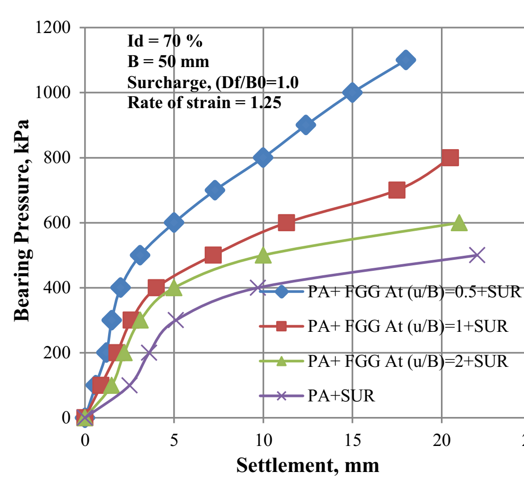

Fig. 13 : Variation of bearing pressure with settlement with coir geotextile (CGT)

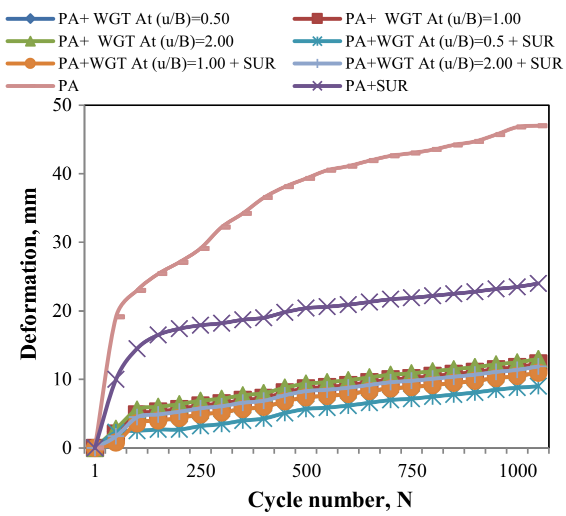

Fig. 14 : Cyclic deformation versus cycle number plot for WGTreinforced pond ash

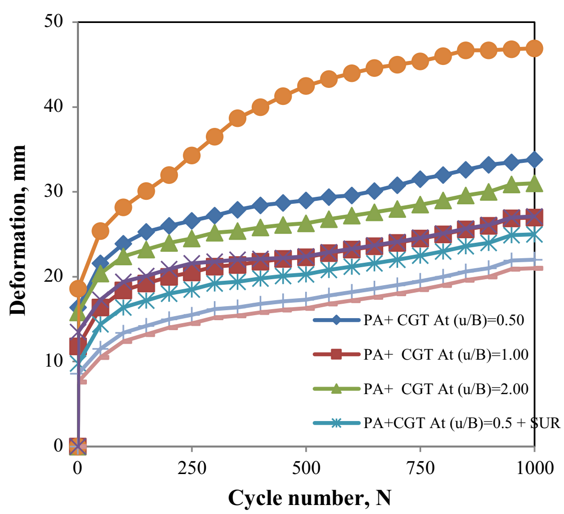

Fig. 15 : Cyclic deformation versus number of cycles for CGT reinforced pond ash

Analysis of the Cyclic Load Test Results

The results of the cyclic load tests are analysed in terms of the apparent resilient modulus (ARM) as defined below:

$$\text{ARM} = \frac{\text{Magnitude of peak cyclic stress applied (kPa)}}{\text{Elastic recoverable component of the cyclic deformation (mm)}}$$

The variation of ARM with cycle number for the pond ash reinforced with WGT and CGT for different (u/B) ratios in the absence and presence of surcharge is depicted in Figs. 16 and 17, respectively.

Based on the analysis of the cyclic load test results, the following observations are made:

1. The total cyclic deformation versus cycle number plots typically depict large deformations in the first few cycles up to a distinct point of inflection followed by a gentle slope. The point of inflection may be indicative of completion of additional fill compaction that is exclusive under cyclic loading conditions. It is indicative of improvement in elastic modulus of the medium. Under the application of a given cyclic stress, the number of cycles required to reach the point of inflection is dependent on the initial elastic modulus of the medium. The pond ash reinforced with lowmodulus CGT required more number of cycles to reach point of inflection and in the process has undergone more total and recoverable deformation than pond ash reinforced with higher-modulus WGT.
2. As it can be seen from Figs. 16 and 17, the apparent resilient modulus of the pond ash reinforced with WGT as well as CGT is found to be increasing as the number of cycles is increasing, but the values are higher for WGT.

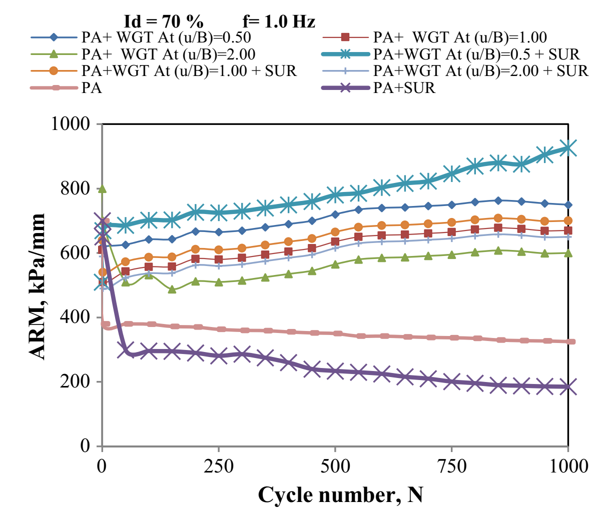

Fig. 16 : Variation of ARM with cycle number for pond ash reinforced with WGT

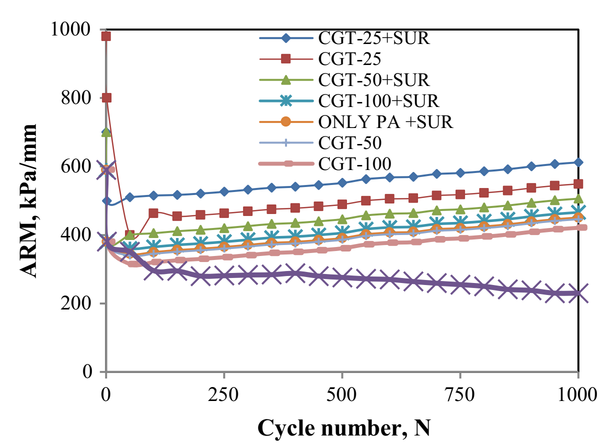

Fig. 17 : Variation of ARM with cycle number for pond ash reinforced with CGT

Laboratory Study at CET

Laboratory studies were reported by Bindu et al. [6] using coir geotextiles of 681 gsm on model tests in a square tank of size 750 mm 9 750 mm 9 750 mm. A schematic diagram of the test setup is shown in Fig. 18. The load was applied through a square plate 20 mm 9 20 mm 9 5 mm. The settlement of the plate was measured using dial gauges, fitted on the plate on either side of the loading shaft.

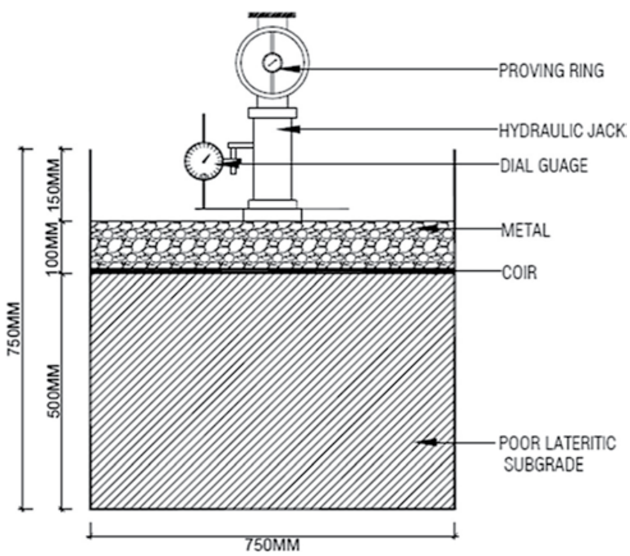

Fig. 18 : Schematic diagram of experimental setup

Soil sample has been compacted to 500 mm into the tank in layers to a dry density of 1.88 g/cc. Over this, 30 mm graded aggregate is filled in two layers, 50 mm each. Four sets of experiments were carried by changing the position of coir-reinforced mats, viz. (i) unreinforced soil sample, (ii) reinforced soil sample with coir above subbase, (iii) reinforced soil sample with coir above subgrade and (iv) reinforced soil sample with coir in the middle of subgrade.

Comparison of various conditions included in Table 4 demonstrates the improvement with coir geotextiles.

Table 4 : Results of unreinforced and coir-reinforced models

Specimen	Failure stress (kN/m^2)
Unreinforced sample	35.70
Coir-reinforced above subgrade	69.85
Coir-reinforced above subbase	93.13
Coir-reinforced in between subgrades	82.27

Field Trials with Coir Geotextiles

Eight rural roads being constructed under PMGSY scheme have been selected for the study [3,7]. The roads had been reinforced with coir geotextile due to the low subgrade CBR values. A subgrade layer of 300 mm thickness was first prepared by roller compaction and the coir geotextile unrolled in the direction of traffic. It was then sufficiently anchored to the subgrade. Geotextile panels are overlapped both side-to-side and end-to-end. The recommended overlaps ranged from 150 to 300 mm, depending on the subgrade strength. The coir geotextiles used were GT 1–681 gsm, GT 2–440 gsm and GT 3–915 gsm. After placing the geotextile, a granular subbase layer of 75 mm thickness and two water-bound macadam layers, each of 75 mm thickness, were constructed, over which the bitumen layer was laid. Except the introduction of the coir geotextile over the subgrades, the rest of the design thicknesses of the different pavement layers were as per the Rural Road Manual (IRC 2000). The roads have been opened to traffic subsequently. The details of the roads are presented in Table 5.

Cross Section of Pavement

In Roads 1–6, coir geotextile is placed on top of the subgrade layer of 300 mm thickness which is of fill material. Then a granular subbase layer of 75 mm and two waterbound macadam layers, each of 75 mm, are laid over the coir geotextiles. The cross section of the pavement is shown in Fig. 19.

Coir geotextile-reinforced Roads 7 and 8 were each of 100 m, and geotextiles were placed at different locations for four different stretches of each 25 m length.

Properties of fill soil in Roads 1 to 6 are presented in Table 6, and those of Roads 7 and 8 are presented in Table 7.

In Roads 1–6, GT 1 coir geotextile was placed, and in Roads 7 and 8 GT 2 and GT 3 were used. The properties of coir geotextile are presented in Table 8.

Typical photographs of roads before construction and during construction are shown in Figs. 20 and 21, respectively.

Performance of Coir Geotextile-Reinforced Pavements

Visual examination of all coir geotextile-reinforced sections showed that they were free from pavement distresses and comparatively in good condition. For the detailed evaluation, the dynamic cone penetrometer test (DCP),Benkelman beam deflection test (BBD) and field CBR (FCBR) tests were conducted on the roads.

Table 5 : Name and details of the roads for field trials in Kerala state

Designation	Name of road	Length (m)	Date of construction
Road 1	Attukal–Pampadi, Trivandrum	150	23/09/11
Road 2	Karikuzhy–Chekidampara, Trivandrum	470	24/0/11
Road 3	Kumbarivila–Kollantemukku, Kollam	1168	16/10/11
Road 4	ANC Mulamootilpadi, Alappuzha	2500	12/03/12
Road 5	Manakodam–Rationkada, Pathanamthitta	750	01/01/13
Road 6	Puthusserikadavu–Kakkathikara, Ernakulam	222	08/12/11
Road 7	Chirakkad–Kumbakad, Trivandrum	100	10/08/08
Road 8	Mangalabharathy–S N Kadavu, Alappuzha	100	15/08/08

Table 6 : Subgrade soil properties of fill soils of Road 1 to Road 6

Properties	Road 1	Road 2	Road 3	Road 4	Road 5	Road 6
LL (%)	42	35	46	41	65	61
PL (%)	25	19	26	19.6	39	29
PI (%)	17	16	20	21.4	26	32
MDD (kN/m^3)	16.87	19.03	16.19	15.99	15.01	15.99
% Silt + clay	42.09	26.58	27.06	58.16	53.20	48.08
Soaked CBR	1.35	2.84	1.41	1.01	1.52	1.28

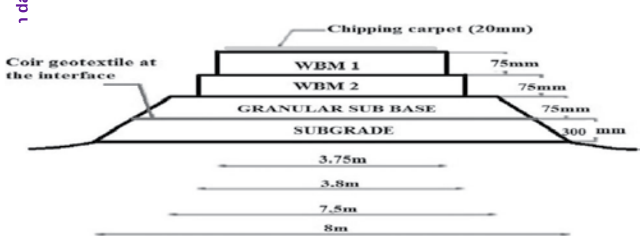

Fig. 19 : Cross section of Roads 1 to 6

Fig. 20 : View of a road during construction

Fig. 21 : Another view of a road during constructions

Table 7 : Soil properties of local soil of Road 7 and Road 8

Sl. No	Soil properties	Road 7	Road 8
1	LL (%)	24	23
2	PL(%)	18	18
3	PI (%)	6	5
4	MDD (kN/m^3)	19.82	21.58
5	Silt ? clay (%)	32	33
6	Soaked CBR	2.1	1.68

Table 8 : Properties of coir geotextile

Properties	GT-1	GT-2	GT-3
Mass/unit area, g/m_2	681	425	915
Opening size, mm	9×12	15×22.5	6×10.5
Thickness, mm	7.16	8.1	8.7
Wide width tensile strength, kN/m			
M/D*	19.8	10.5	24.8
CM/D#	18.8	7.1	17.5

*Machine direction, # cross machine direction

Dynamic Cone Penetrometer Test (DCP)

DCP test is conducted to estimate the penetration rate when an 8 kg hammer is allowed to fall freely through a constant height. The testing procedure adopted is based on ASTM D6951/D6951M-09. The depth of penetration is taken up to 300 mm.

DCP tests were conducted on the roads during dry and wet season after 4 to 5 years of construction. The variation of depth of penetration of the cone with number of blows during dry season is plotted, and typical results are shown in Figs. 22a, b and 23. Designations like GT1, GT2, GT3, etc., refer to various locations on a coir-reinforced road, and WOGT1, WOGT2, WOGT3, etc., refer to various locations on a road without coir geotextile.

It is evident that the penetration/blow for reinforced roads is less than that for the unreinforced section. The DCP indices are calculated which is the slope of the variation of penetration with the number of blows curve and are given in Table 9.

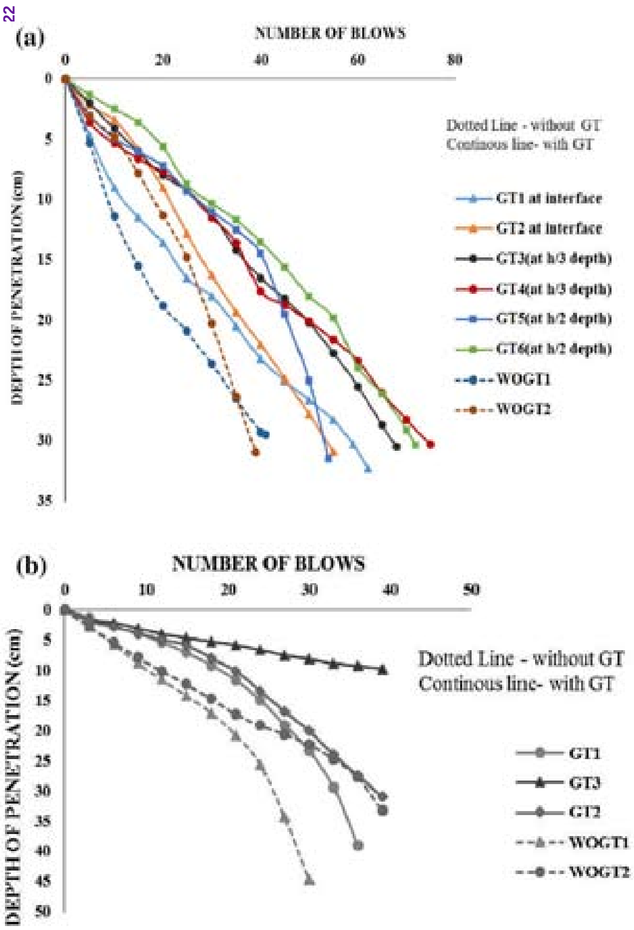

Fig. 22 : a Variation of penetration with number of blows for Road 5. b Variation of penetration with number of blows for Road 7

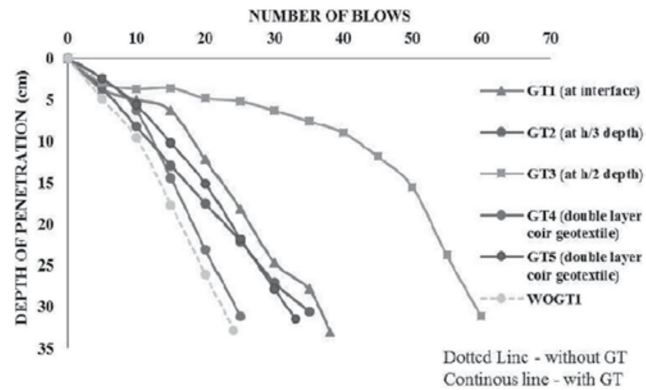

Fig. 23 : Variation of penetration with number of blows for Road 8

Table 9 : DCP indices obtained during dry season

Average DCP indices (penetration cm per blow)			
	Test road without geotextile	Test road with geotextile	% decrease in DCPI
Road 1	0.87	0.63	27.5
Road 2	0.76	0.69	9.2
Road 3	0.67	0.42	37.3
Road 4	0.52	0.33	36.5
Road 5	0.95	0.69	27.4
Road 6	0.87	0.38	56.3
Road 7	0.73	0.48	38.8
Road 8	1.39	0.83	47.9

DCPI for coir geotextile-reinforced section is found to be less than that of the unreinforced section, and the percentage reduction varies from 27.4 to 56.3% except for Road 2 which is 9.2%. It can be said that improvement due to coir geotextile is less when the soil has considerable strength. For Road 7 and Road 8, out of the four different positions of coir geotextile installation, the DCPI obtained for the stretch having geotextile at the interface of subgrade and subbase is the minimum. Hence, this is the optimal position. For the section having two coir layers with a local clay, the DCPI is found to be less than that of the unreinforced section but greater than that of the single-layer geotextile reinforcement with fill soil. Therefore, it can be said that in the absence of adequate fill soil, local soil with two layer of geotextile can be used to stabilize the pavement.

Similarly, results of DCP tests conducted during wet season and the DCP indices obtained are presented in Table 10. There is a considerable decrease in the DCP indices of coir geotextile-reinforced section than that of the unreinforced section.

Table 10 : Average DCP indices obtained during wet season

Sl. No.	Avg. DCP indices (penetration/blow)		% Decrease
	Without geotextile	With geotextile	
Road 1	1.29	0.569	56
Road 5	2.43	1.27	48
Road 7	1.78	0.86	53
Road 8	2.42	0.64	81

Benkelman Beam Deflection Test

Performance of flexible pavements is closely related to the elastic deflection of pavement under the wheel loads. The rebound deflection of the pavement is determined using Benkelman beam in accordance with the procedure given in IRC 81-1997.

The rebound deflection of the coir geotextile-reinforced section as well as the unreinforced section is presented in Table 11. The percentage decrease in BBD rebound deflection of the reinforced section ranges from 18 to 80%. The section with coir geotextile at the interface shows minimum rebound deflection and hence the optimum position for geotextile installation.

Table 11 : BBD test results after 4 to 5 years of construction

Name of road	Without coir GT	With coir geotextile	% Decrease in rebound deflection
Road 1	0.31	0.06	80
Road 4	1.58	1.29	18
Road 5	1.84	1.21	34
Road 6	0.12	0.08	33
Road 7	5.66	1.97	65
Road 8	3.68	2.38	35

BBD value of coir geotextile-reinforced and unreinforced roads monitored over 4 to 5 years shows that the variation in the BBD value of the reinforced and unreinforced roads is large immediately after construction and it reduces with time. In other words, with time the unreinforced section may reach the value of the reinforced section.

Field CBR Test

Field CBR values conducted by DCP on coir geotextilereinforced and unreinforced roads after 4 to 5 years of construction are presented in Table 12.

The percentage increase in CBR values thus ranges from 9 to 127%.

Table 12 : Field CBR values (through DCP)

Sl. No.	Field CBR values (%)		% Increase in CBR
	With geotextile	Without geotextile	
Road 1	72	66	9
Road 4	49	33	48
Road 5	36	22	64
Road 6	89	64	39
Road 7	50	22	127
Road 8	73	39	87

Other Field Testing

Work was also carried out to assess the pavement condition by Merlene test and roughness. These could not be presented here, but on the whole there is performance with coir geotextiles.

OTHER RELATED STUDIES

Through extensive laboratory and field studies on Rural Roads of Tamil Nadu, conducted by National Institute of Technology, Tiruchirappalli, Samson Mathew (2018) concluded the following:

1. The CBR value of the coir reinforces specimen reached the highest value of 9% (virgin soil CBR value 2.5%) when the coir geotextile was placed just above subgrade.
2. Plate load tests conducted on coir-reinforced pavements showed a percentage increase of 127% in load carrying capacity.
3. Provision of a layer of geotextile at the interface between subgrade and subbase reduces the deformation by 40%, which in turn results in the reduction in subbase thickness required.

CONCLUSIONS

From the results of monotonic and cyclic behaviour of clayey soils and pond ash in model test tanks, it is evident that the overall engineering behaviour with inclusion of coir geotextiles improves significantly.

The field studies conducted on rural roads in Kerala and Tamil Nadu for over 6 years clearly established the improvement in pavement behaviour with coir geotextiles at the subgrade granular subbase interface.

On the whole, it is evident that coir geotextiles will be a valuable asset for use in rural roads on soft and weak clayey subgrade soils and have immense potential for application in rural roads.

Acknowledgements

I wish to profusely thank the following researchers whose work is included in this paper: Professor K. Balan, Professor Rakesh Dutta, Professor MVS Sreedhar and all the associated engineers and students, who have diligently carried out this work. Special thanks are due to CCRI, Kalavoor, The Kerala State Coir Corporation, and the Rural Road Development Department, Government of Kerala.

Available BIS Codes on Coir Geotextiles Coir Felt—Specification, 2003, IS 15340.Natural fibre geotextiles (jute geotextile and coir Bhoovastra)—Methods of test, 2008, IS 15868: Parts 1-6.Open weave coir Bhoovastra—Specification, 2008, IS 15869.Use of coir geotextiles (coir Bhoovastra) in unpaved Roads—Guidelines, 2009, IS 15871.Application of coir geotextiles (coir woven Bhoovastra) for rain water erosion control in roads, railway embankments and hill slopes—Guidelines, 2009, IS 15872.

REFERENCES

1. Balan K (1995) Studies on the engineering behaviour and uses of geotextiles with natural fibres, Ph.D. Thesis, IIT Delhi
2. Rao GV, Balan K (2000) Coir Geotextiles. In: Rao GV, Balan K (eds) A perspective, coir geotextiles—emerging trends. The Kera1a State Coir Corporation, Alappuzha, pp 5–14
3. Rao GV, Sheela EY, Joseph M, Sayida MK, Bindhu BH, Sajikumar PR (2016) Rural roads with coir geotextiles—a performance appraisal. In: Proceedings of the international coir fair and seminar, Alappuzha, Kerala
4. Rao GV, Dutta RK (2006) Coir geotextiles in rural roads. Highw Res Bull 74:9–15
5. Venkattappa Rao G, Sreedhar MVS (2012) Monotovic and cyclic response of pond ash reinforced with coir geotextile. Geosynthetics Asia, GA-2012, Bangkok 1, pp 907–915
6. Bindu BH, Sheela EY, Mariamma J, Sayida MK (2014) Study on the functional performance of coir geotextile reinforced flexible pavements. In: Proceedings of IMMM 2014 CET, Thiruvananthapuram
7. Anupriya SG, Sheela EY, Sayida MK, Ajin K (2016) Study on the long term performance of coir geotextile reinforced flexible pavements. In: Proceedings of NCTT 2016, CET, Thiruvananthapuram

BEARING CAPACITY OF GEOSYNTHETIC REINFORCED CNS SOIL BED ON CLAYEY SOIL WITH INCLINED REINFORCEMENT CONSIDERING KINEMATICS

Rajashekar Reddy Palvaie[1], G.V.N Reddy[2] and Sai Baba Reddy E[3]

ABSTRACT

The conventional method of placing polymeric Reinforcement in Foundation Beds is in the form of horizontal layers to resist the applied force by mobilization of bond resistance at the interface between reinforcement and soil limited by ten-sile strength of its own. Present work analyses geosynthetic reinforcement placed inclined from the edge of the footing towards the free end at an inclination varying between 0 to 10^0 and calculated the bearing capacity considering the effect of kinematics, i.e., The effect of transverse resistance in addition to the axial resistance of the inclined reinforcement to-gether with shear resistance of soil bed. The variation of bearing capacity with angle of shearing resistance of soil bed, relative stiffness of soil, transverse deformation, length of reinforcement, intensity of surcharge also studied in addition to the inclination of reinforcement. The improvement in normalised bearing capacity ratio considering transverse resistance of the inclined reinforcement is significant when compared with the horizontal reinforcement.

***Keywords** : Reinforced Foundation Beds, Normalised Bearing Capacity, Transverse Resistance, Inclination of Rein-forcement, Relative Stiffness of soil.*

1. INTRODUCTION

Geosynthetic reinforcement placed in the reinforced foundation bed resist the forces applied on it by tensile force mobilised in it due to interfacial friction between soil and reinforcement. The common trend in reinforced foundation bed is to place the reinforcement in horizontal layers and for the design of reinforced soil foundation beds, horizontal pull out resistance of reinforcement is considered. In the conventional method of slope stability and analysis of reinforced wall orientation of reinforcement in the proximity of failure surface is usually assumed in axial di-rection (Flower [1982], Jewell [1992], Sobhi and Wu [1996], Bergado et al., [2000], Abdi and Zandieh [2014]). Whereas some researchers assumed orientation of reinforcement in a direction tangential to the slip surface Quast [1983] showed that increase in pull out resistance due tangential orientation of reinforcement to slip surface. Similarly, effect of other orientations between these two extremes were considered by Rowe and Soderman [1984], Bonaparte and Christopher [1987]However, localized mobilization of reinforcement force is dependent on the kin-ematics of failure of reinforced structures. The kinematics of failure is assumed such that failure surface intersects the reinforcement obliquely. Michalowski & Shi [1985] used kinematic approach of limit analysis for calculating the pressure of footing over a double layer foundation soil and found that limit pressure under foundation depends not only on the angle of shearing resistance of sand, surcharge and thickness of sand layer but also on cohesion of insitu clay layer. Umashankar and Madhav [2003], Madhav and Manoj [2004], analysed the rein-forced soil structure considering the kinematics and proved that reinforcement subjected to transverse pull mobilizes additional bond resistance than the axial pull out. Response of inextensible reinforcement subjected to oblique pull at one end studied by Sahu [2007] by considering the rigid plastic response of soil reinforcement interface and linear normal stress deformation of fill material. Horizontal component of oblique pull out force is 50% more than that of axial pull out capacity for the case with angle of shearing resistance of fill material equal to 30°. Analytical model proposed by Sahu [2007] extended by Sahu and Hayashi [2009] assuming Shear-stress displacement of geosynthetic reinforcement-soil interface and non-linear response for normal stress deformation of sub-grade to analyze the behavior of extensible reinforce-ment to oblique pull. Narasimha Reddy et al., [2009] and Gao et al., [2014] developed an analytical solution considering oblique pull out of reinforcement in the design of reinforced earth walls subjected to seismic and static loads. Patra and Sahu [2012] considered Pasternak model instead of Winkler model for representation of sub-grade material as Pasternak model

1. Research Scholar, JNTUH, Hyderabad, India

2. Professor, JNTUH, Hyderabad, India

3. Principal and Professor, JNTU, Hyderabad, India

provides more realistic response of the pullout behavior. It is also observed that with increase in shear stiffness, displacement profile of the reinforcement become more uniform and bending of reinforcement reduces leading to reduction in normal stresses resulting in mobilization of smaller values of tension in the reinforcement. Kumar and Madhav [2011] analyzed reinforced soil wall with geo-textile reinforcement 0° to 10° downward inclination with horizontal and found that factor of safety against pull out increased due to increase in normal stress acting on reinforcement. Hariprasad et al., [2018] developed test chamber with arrangement to perform transverse pull out resistance factor for smooth metal strip reinforcements corresponding to different transverse displacement of the reinforcement and found increase in pullout resistance. In this paper, it is proposed to study the increase in bearing capacity due to mobilization of shear stress resulting from additional normal stress acting below the reinforcement considering transverse deformation. Hence, in this paper a parametric study has been carried out to study the effect of kinematics (transverse deformation) on inclined reinforcement in soil bed in improving bearing capacity.

2. PROBLEM DEFINITION AND FORMULATION

A strip footing with width, B resting on the surface of CNS Soil bed overlying soft homogeneous clay, having cohesion c, is considered as shown in Fig.1. The distance between base of footing up to interface of CNS soil bed and clay is H. Single inextensible layer of geotextile re-inforcement having length, Lr is placed in the CNS soil bed at a depth u from the bottom of footing and is inclined at an angle α with horizontal such that tip at free end of geotextile is at a depth of H = [u+(Lr-B/2)sinα]. Angle of shearing resistance and unit weight of CNS Soil bed are ϕ and γ respectively and cohesion is neglected. Interface friction angle between soil and reinforcement is ϕ_r and T_r is the tension developed in the reinforcement. Above Fig.1 shows the deformations of the CNS soil column and geo-textile reinforcement due to consideration of punching shear failure of the footing. Geotextile reinforcement is originally placed inclinedly represented by the line PQRS and deformed to the new position by PQQ'R'RS. To simulate the embedded footing, a uniform surcharge pressure

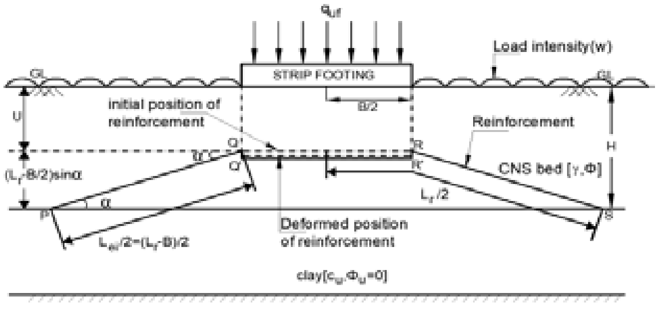

Fig. 1 : Definition sketch

of w is assumed to be acting on the reinforced foundation bed. Reinforcement is subjected to overburden pressure varying from γu at the edge of the footing to γH at the free end of reinforcement based on the location. Bottom of footing is assumed as rough and tensile strength of the re-inforcement is assumed to be less than the rupture strength of reinforcement. Failure is initiated by the punching mode in the topsoil bed. Full shear resistance mobilization along geotextile soil interface is assumed.

3. METHOD OF ANALYSIS

3.1 Bearing Capacity of Cohesive Non-Swelling Soil Bed On Clay Soil:

Meyerhof's(1974) solution for bearing capacity of the embedded strip footing placed at a depth D resting on dense sand bed overlying soft homogenous clay considering punching mode of shear failure is used and is given by

$$q_{cns} = cN_c + \frac{\gamma H^2}{B}\left(1+\frac{2D}{H}\right)k_s tan\phi + \gamma D \leq 0.5\gamma BN_r] \quad ...(1)$$

For a strip footing resting on top of sand bed D= 0,

$$q_{cns} = cN_c + \frac{\gamma H^2}{B}K_s tan\phi \leq 0.5\gamma BN_r \quad ...(2)$$

Where,

N_c = Bearing capacity factor for clay layer. γ = unit weight of CNS soil. K_s = Coefficient of punching shear. ϕ = friction angle of CNS soil. N_γ = bearing capacity factor with respect to friction angle (ϕ) of CNS bed.

K_s can be obtained using chart provided by Meyerhof & Hanna,(1978) and its value depends on angle of shearing resistance of soil ϕ, undrained shear strength of clay, c, bearing capacity ratio q_2/q_1, where q_1 and q_2 are ultimate bearing capacities of soil bed and soft homogeneous clay respectively.

Non-dimensionalizing equation (2) with undrained cohesion of clay, *c*

$$q_{cns}{}^{*} = N_c + \left(\frac{\gamma B}{c}\right)\left(\frac{H}{B}\right)^2 K_s tan\phi \quad ...(3)$$

3.2 Bond Resistance of Geotextile Reinforcement Placed Inclined in CNS Soil Bed:

It is considered that due to weight of structure, strip footing along with CNS soil column below the footing moves down due to punching effect and shear stresses are developed on both sides of the soil column. Bond resistance mobilizes at the interface of soil and geo-textile. Geotextile reinforcement is subjected to overburden pressure in-creasing from γu at edge of footing to γu+γ[(Lr-B)/2] sinα at the free end (i.e., tip of inclined reinforcement). Vertical stress and tension developed in the reinforcement are cal-culated for average depth of reinforcement, u_{avg}

$$u_{avg} = \frac{[u]+[u+\left(\frac{Lr}{2}-\frac{B}{2}\right)sin\alpha]}{2} \quad ...(4)$$

3.3 Bond Resistance Developed due to Reinforcement:

Overburden pressure acting on geotextile reinforcement is

$$q = \gamma u_{avg} + w$$

$$q = \gamma\left(u + \frac{1}{2}\left[\left(\frac{L_r}{2} - \frac{B}{2}\right) sin\alpha\right]\right) + w \qquad ...(5)$$

Stresses normal, qn and tangential, qt to the alignment of geotextile reinforcement are resolved as shown below

$$q_n = \left[\gamma\left(u + \frac{1}{2}\left[\left(\frac{L_r}{2} - \frac{B}{2}\right) sin\alpha\right]\right) + w\right] cos\alpha \qquad ...(6)$$

$$q_t = \left[\gamma\left(u + \frac{1}{2}\left[\left(\frac{L_r}{2} - \frac{B}{2}\right) sin\alpha\right]\right) + w\right] sin\alpha \qquad ...(7)$$

Tangential stress, q_t offers direct resistance against pull-out of reinforcement and due to normal stress qn an additional resistance $q_t tan\phi_r$ mobilized.

Total pull out resistance mobilized,

$$T_r = 2(q_n\, L_{ei}\, tan\phi_r) + 2(q_t L_{ei})$$

Where,

Effective length of inclined reinforcement beyond edge of footing.

$$\mathrm{L}_{ei} = (\mathrm{L}_r - \mathrm{B}) = 2\left(\frac{L_r}{2} - \frac{B}{2}\right)$$

Axial tensile force developed in the reinforcement for an effective length, Lei beyond width of footing due to interface shear resistance between reinforcement and soil.

$$T_r = 2\left\{[\gamma\left(u + \frac{1}{2}\left[\left(\frac{L_r}{2} - \frac{B}{2}\right) sin\alpha\right]\right) + w]cos\alpha].2\left(\frac{L_r}{2} - \frac{B}{2}\right).tan\phi_r\right\} + 2\left\{[\gamma\left(u + \frac{1}{2}\left[\left(\frac{L_r}{2} - \frac{B}{2}\right) sin\alpha\right]\right) + w]sin\alpha].2\left(\frac{L_r}{2} - \frac{B}{2}\right)\right\} \qquad ...(8)$$

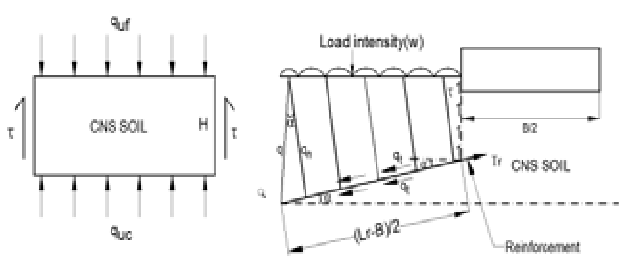

Fig. 2 : Stresses on soil column and inclined reinforcement

Bond resistance mobilised per width of footing

$$\frac{T_r}{B} = \frac{4}{B}\left[\gamma\left(u + \frac{1}{2}\left[\left(\frac{L_r}{2} - \frac{B}{2}\right) sin\alpha\right]\right) + w\right]\left(\frac{L_r}{2} - \frac{B}{2}\right)\{tan\phi_r\ cos\alpha + sin\alpha\} \qquad ...(9)$$

Bearing capacity of CNS soil bed reinforced with inclined reinforcement on soft homogeneous clay is given by

$$q_{uir} = cN_c + \frac{\gamma H^2}{B} K_s \tan\phi + 4\left\{\gamma\left(\frac{u}{B} + \frac{1}{2}\left[\left(\frac{Lr}{2B} - \frac{1}{2}\right) sin\alpha\right]\right) + \frac{w}{B}\right\}\left(\frac{Lr}{2B} - \frac{1}{2}\right)(tan\phi_r\ cos\alpha + sin\alpha) \qquad ...(10)$$

Normalizing the above equation with *c*

$$q_{uir}{}^{*} = N_c + (\frac{\gamma B}{c})(\frac{H}{B})^2 K_s tan\phi + 4\{\frac{\gamma B}{c}(\frac{u}{B} + \frac{1}{2}\ [(\frac{Lr}{2B} - \frac{1}{2})sin\alpha]) + \frac{w}{c}\}\left(\frac{L_r}{2B} - \frac{1}{2}\right)(tan\phi_r\ cos\alpha + sin\alpha) \qquad ...(11)$$

3.4 Effect of Transverse Pull:

Punching mode of shear failure is considered for the esti-mation of bearing capacity of the double layered soil con-sidering the kinematics of failure. As the footing pushes through the soil layer soil column beneath the footing moves down along with reinforcement.

This downward movement mobilizes shear stresses along the edges of soil column and causes the geotextile rein-forcement to be pulled down resulting in the development of additional normal stresses at the bottom of the rein-forcement (Fig.3). Additional bond resistance mobilised due to transverse pull improves the pull-out resistance of reinforcement. Analysis is carried out assuming that full bond resistance is mobilized along the soil- geotextile in-terface and the response of the soil to the transverse dis-placement is linear.

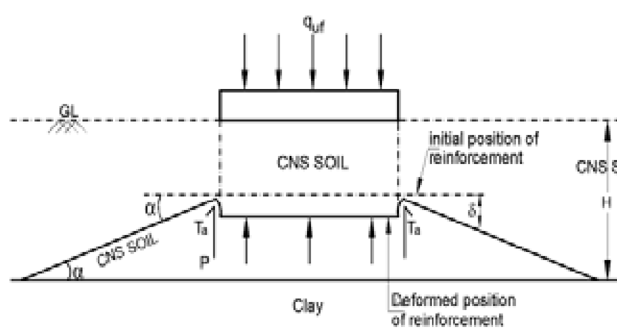

Fig. 3 : Additional stress developed in the inclined rein-forcement due to transverse force

For the analysis of sheet reinforcement subjected to transverse force/displacement, the work carried out by Umashankar and Madhav (2003) to estimate the additionally mobilized resistance is extended. A transverse displacement, (W_L) (Fig. 4) of the reinforcement layer at the edge of the footing is considered to estimate additionally mobilized resistance. As a result of transverse displacement, W_L of the reinforcement, upward resisting force P gets developed. The pullout force in the reinforcement increases due to transverse displacement.

To calculate the resisting forces developed due to transverse displacement of the inclined geotextile reinforcement layer, equations 12 &13 are used.

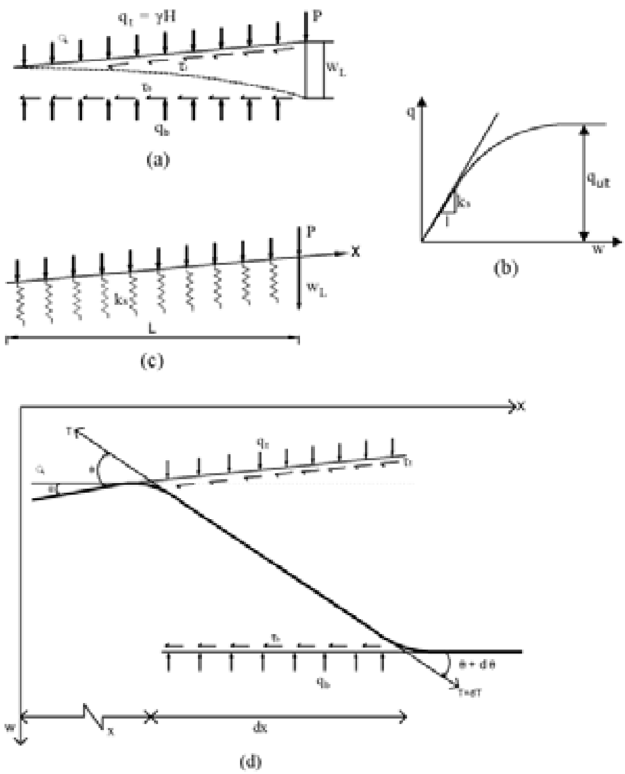

Fig. 4 : (a) Deformed profile (b) normal stress-displacement response of soil (c) Idealization of soil (d) Forces acting on infinitesimal element

Mobilized tension in the reinforcement due to additional normal forces, P is calculated as

$$T = 2\gamma u_{avg} L_{ei} tan\phi_r + P \sec\alpha \, tan\phi_r \quad ...(12)$$

Where, P is the transverse force mobilized in geotextile reinforcement layer due to transverse displacement W_L at the intersection, P is calculated using the following equation.

$$P = \gamma u_{avg} L_{ei} P^* \quad ...(13)$$

Where P* is the normalized transverse force in geotextile layer of length L_{ei} placed at a depth u from bottom of footing in the soil bed of relative stiffness, $\mu\left(\frac{k_s L}{\gamma H}\right)$, subjected to transverse force P due to transverse displacement, w_L, at the edge of footing extending the equation de-veloped by Umashankar and Madhav (2003).

The variation of normalised transverse force P* with nor-malised displacement . / is shown in Fig. 5, for ϕ=30^0. For low subgrade stiffness factor (μ) <1000, implying soft Soil, shorter length of reinforcement or large depth of embedment, transverse force increases linearly with nor-malised displacement. For μ > 1000, larger forces are re-quired to mobilize larger displacements. Reinforcement placed at shallow depth or longer reinforcement tends to deform significantly requiring mobilization of greater forces.

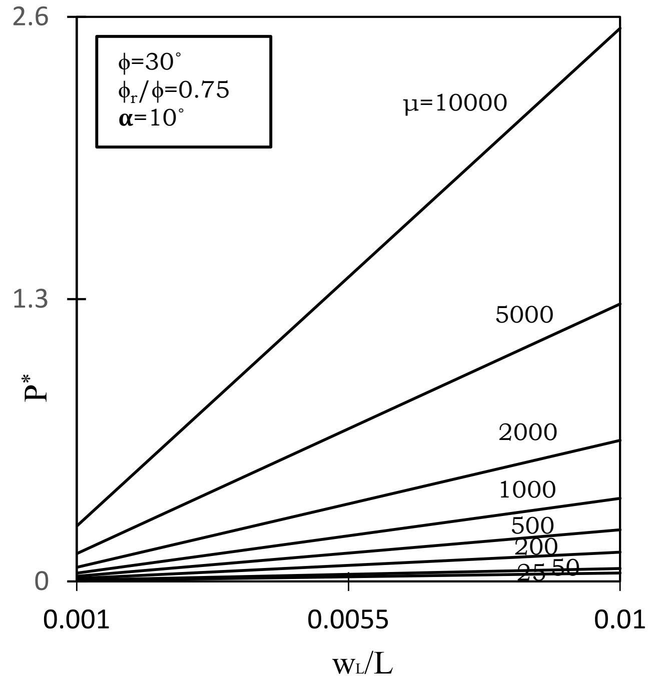

Fig. 5 : Variation of normalised transverse force, P* with normalised displacement, (W_L/L)- Effect of stiffness of soil. (Umashankar and Madhav, 2003).

The bearing capacity of the CNS bed with inclined rein-forcement resting on homogeneous clay soil is the sum of bearing capacity of clay layer, shear resistance mobilized in CNS bed, axial resistance of inclined reinforcement and additional resistance mobilized there in due to kinematics (transverse displacement and additional bond resistance mobilized due to kinematics).

$$q_{urik} = cN_c + \frac{\gamma H^2}{B} K_s \tan\phi + 4\left\{\gamma\left(\frac{u}{B} + \frac{1}{2}\left[\left(\frac{Lr}{2B} - \frac{1}{2}\right)\sin\alpha\right]\right) + \frac{w}{B}\right\}\left(\frac{Lr}{2B} - \frac{1}{2}\right)(\tan\phi_r \cos\alpha + \sin\alpha)(1 + T^* + P^*) \quad (14)$$

Non dimensionalizing the above equation with *c* gives

$$q_{urik}^* = N_c + \left(\frac{\gamma B}{c}\right)\left(\frac{H}{B}\right)^2 K_s \tan\phi + 4\left\{\frac{\gamma B}{c}\left(\frac{u}{B} + \frac{1}{2}\left[\left(\frac{Lr}{2B} - \frac{1}{2}\right)\sin\alpha\right]\right) + \frac{w}{c}\right\}\left(\frac{Lr}{2B} - \frac{1}{2}\right)(\tan\phi_r \cos\alpha + \sin\alpha)(1 + T^* + P^*) \quad (15)$$

Increase in ultimate bearing capacity by using geotextile reinforcement in soil bed is quantified through a non-dimensional parameter, the normalized bearing capacity ratio.

The normalized bearing capacity ratio, q_{cns}* is the ratio of bearing capacity of CNS bed overlying homogeneous clay layer to the undrained shear strength of clay.

q_{ur}* is the ratio of bearing capacity of CNS bed with rein-forcement placed horizontally considering axial tension in the reinforcement overlying clay to that of undrained shear strength of clay.

q_{uri}* is the ratio of bearing capacity of geotextile reinforced CNS bed with reinforcement placed inclinedly considering axial tension in inclined reinforcement overlying clay to that of undrained shear strength of clay.

q_{urhk}* is the ratio of the bearing capacity of the CNS bed with reinforcement placed horizontally considering effect of transverse force considering kinematics in addition to axial tension in the reinforcement overlying clay to that of undrained shear strength of clay.

qurik* is the ratio of bearing capacity of CNS bed with re-inforcement placed inclinedly considering the effect of transverse force in addition to axial tension in inclined re-inforcement overlying clay to that of undrained shear strength of clay. This ratio quantities the contribution of the transverse force mobilized as a consequence of kine-matics over and above the contributions of CNS bed and axial force mobilised in inclined reinforcement to the bearing capacity of footing.

Meyerhof's (1974) punching mode of failure for the thin dense sand bed overlying homogeneous clay is used as the basis for the analysis. As the reinforcement moves along with the soil column, shear stresses are developed on ei-ther side of soil column, bond resistance mobilised at the interface of soil and reinforcement as the upward normal force acts on bottom of reinforcement due to transverse displacement/ force at the edge of the footing. Inclined re-inforcement enhances bearing capacity due to the com-bined effect of overburden pressure acting on reinforce-ment and mobilization of additional shearing resistance due to normal stress acting on the reinforcement. The pro-posed bearing capacity equation for the strip footing on CNS soil bed reinforced with inclined reinforcement over homogenous clay layer considers the sum of bearing ca-pacity of bottom clay layer, mobilised shearing resistance in the CNS bed, pull out resistance of inclined reinforce-ment and additional shear resistance mobilised at bottom of reinforcement caused by transverse pull.

4. RESULTS AND DISCUSSION

Bearing capacity of strip footing resting on CNS soil bed with inclined reinforcement considering kinematics is studied. The parameter related to CNS soil bed on clay (u/B, ϕ, H/B, γB/c) and interface shear resistance between geotextile layer and soil ϕ_r, (Lr-B/2) length of reinforce-ment beyond edge of footing and α are considered for par-ametric study.

It is assumed that reinforcement will not fail in rupture and pull out of reinforcement is the only possible mode of failure. Results are illustrated in graphical form for the following range of non-dimensional parameters, H/B=0.5, γB/c =0.9 to 3.6,w_L =0.001 to 0.01, μ =50 to 10000 in ad-dition to that α=0,5°,10°, L_r/B= 2.5,3.0,3.5,4.0, ϕ_r/ϕ = 0.67, 0.75, 1.0, w/c =0,0.5,1.0,2.0 are studied. Effect of these parameters on bearing capacity is quantified in this paper for different values of α and compared nor-malised bearing capacity of soil bed with reinforcement placed inclined with that of horizontal reinforcement.

4.1 Effect of Various Improvement Techniques:

Variation of normalised bearing capacities q_{cns}*/ q_{ur}*/ q_{uri}*/q_{urhk}*/q_{urik}* with inclination of reinforcement, α for w/c=0, ϕ=30˚, ϕ_r/ϕ=0.75, L_r/B=3, H/B= 0.5,u/B= 0.15, γB/c= 1.8, μ=1000, (W_L/L) =0.01 are represented in Fig.6. Normalised bearing capacity of CNS bed with inclined re-inforcement on clay considering kinematics, q_{uirk}* in-creases with increase in inclination of reinforcement due to combined effect of increase in overburden stress acting on reinforcement beyond the edge of footing, mobilization of additional shear resistance due to consideration of kinematics.

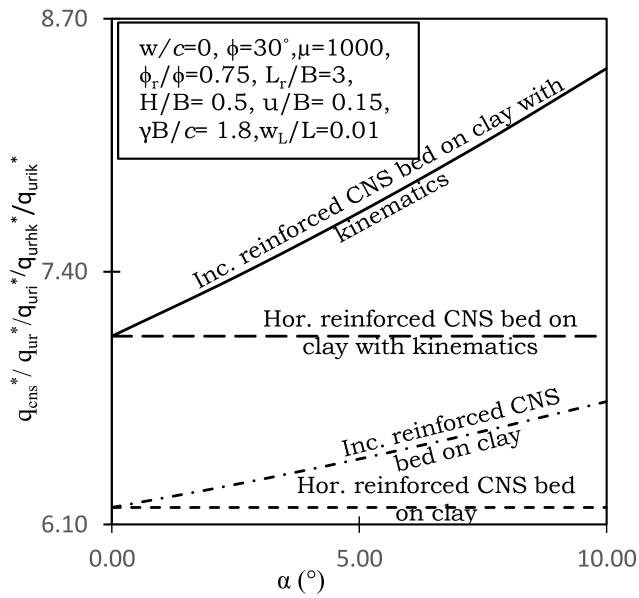

Fig. 6 : Variation of Normalised bearing capacities versus inclination of reinforcement α-Effect of various techniques

Additional bond resistance is mobilised along the bottom of reinforcement-soil interface, owing to additional normal stress acting beneath reinforcement leading to an increase in pull out resistance. q_{urik}* increases 36.3%,25.4%,19.4%, when compared with horizontally placed geotextile reinforced soil bed on clay, inclined re-inforced soil bed on clay and soil bed on clay reinforced horizontal considering kinematics respectively.

4.2 Effect of Relative Stiffness of Soil Fill

Variation of normalised bearing capacity, qurik* with incli-nation of reinforcement, α in CNS bed for w/c=0, ϕ=30˚, ϕ_r/ϕ=0.75, L_r/B=3, H/B= 0.5, u/B= 0.15, γB/c= 1.8, wL/L=0.01 is shown in Fig.7. qurik * increases non-linearly with increase in inclination of the reinforcement, α from

7.07 to 8.44 an increase of 19.4% for increase in α from 0 to 10° for μ=1000 due to the combined effect of increase in normal stress acting on reinforcement beyond the edge of footing and mobilization of additional shear resistance. qurik* increases from 7.24 to 8.07 an increase of 11.5% for an increase in μ from 50 to 2000,at α=5°.With increase in stiffness of subgrade the transverse force required to mobilize transverse displacement increases, additional bond resistance is mobilised due to transverse displacement.

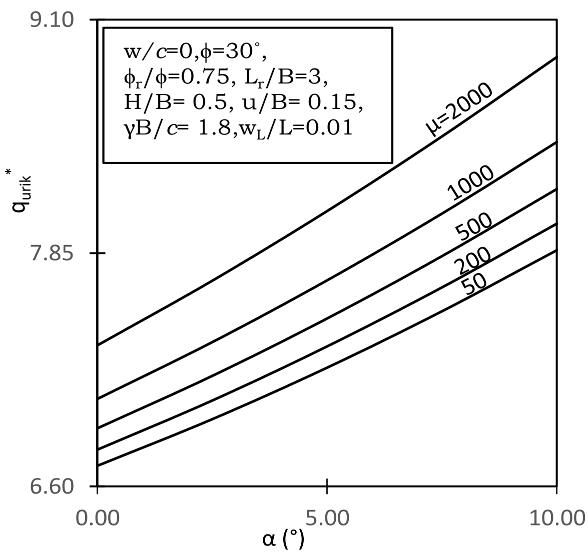

Fig. 7 : Variation of normalised bearing capacity, qurik* versus inclination of reinforcement -Effect of Relative stiffness (μ)

4.3 Effect of Transverse Deformation

Variation of normalised bearing capacity q_{uirk}* with inclination of reinforcement α in CNS bed for w/c=0, ϕ=30˚, ϕ_r/ϕ=0.75, Lr/B=3, H/B= 0.5, u/B= 0.15, γB/c= 1.8, μ=1000 for different valves w_L/L of are represented in Fig.8.

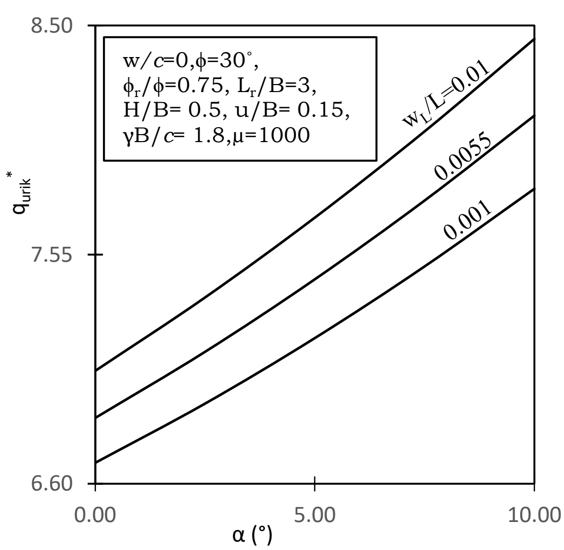

Fig. 8 : Variation of q_{urik}* versus inclination of reinforcement, α-Effect of w_L/L

For w_L/L=0.0055, variation of normalised bearing capacity qurik* increases from 6.87 to 8.13 an increase of 18.4% for an increase of α from 0 to 10° due to combined effect of overburden stress acting on reinforcement and development of additional tangential stress mobilized due to normal stress acting beneath reinforcement. For 5° incli-nation of reinforcement, q_{urik}* increases from 7.20 to 7.70 an increase of 7% for increase of w_L/L from 0.001 to 0.01.The increase in transverse displacement of reinforcement increases the normal stresses acting on reinforcement. Additional bond resistance mobilized due to normal stress increase the bearing capacity.

4.4 Effect of Angle of Shearing Resistance

Variation of normalised bearing capacity q_{urik}* with inclination of reinforcement, α for w/c=0, ϕ_r/ϕ=0.75, Lr/B=3, H/B= 0.5, u/B= 0.15, γB/c= 1.8, μ=1000, wL/L=0.01 for various values of ϕ are illustrated in Fig. 9.

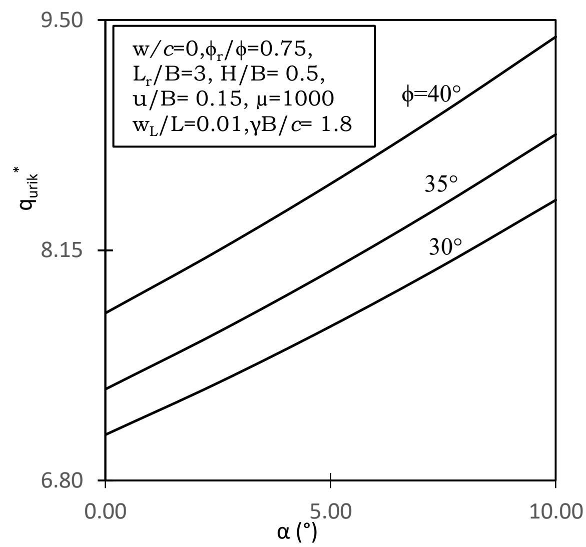

Fig. 9 : Variation of qurik* versus Inclination of reinforcement α-Effect of ϕ.

q_{urik}* increases from 7.34 to 8.83 an increase of 20.3% for an increase of α from 0 to 10° for ϕ=35° due to combined effect of increase in over burden pressure acting on reinforcement, additional bond resistance mobilised below reinforcement along soil-geotextile interface due to in-creased normal stress acting beneath reinforcement.

For an inclination of 5°, q_{urik}* increases from 7.70 to 8.54 an increase of 11% with increase of ϕ from 30° to 40° due to mobilization of frictional component of full out re-sistance.

4.5 Effect of Angle of Interface Friction

Variation of normalised bearing capacity q_{urik}* with α for w/c=0, ϕ=30˚, L_r/B=3, H/B= 0.5, u/B= 0.15, γB/c= 1.8, μ=1000 and w_L/L=0.01 for different values of ϕ_r/ϕ=are shown in Figure 10.

q_{urik}* increases from 7.07 to 8.44 an increase of 19.4% for ϕ_r/ϕ=0.75 and an increase in α from 05 to 10° due to combined effect of overburden pressure acting on reinforcement and bond resistance mobilised due to normal stress acting on reinforcement. For an inclination of 5°, q_{urik}* in-creases from 7.54 to 8.24 an increase of 9.3% with in-crease in ϕ_r/ϕ from 0.67 to 1 due to increase in interface roughness of geotextile.

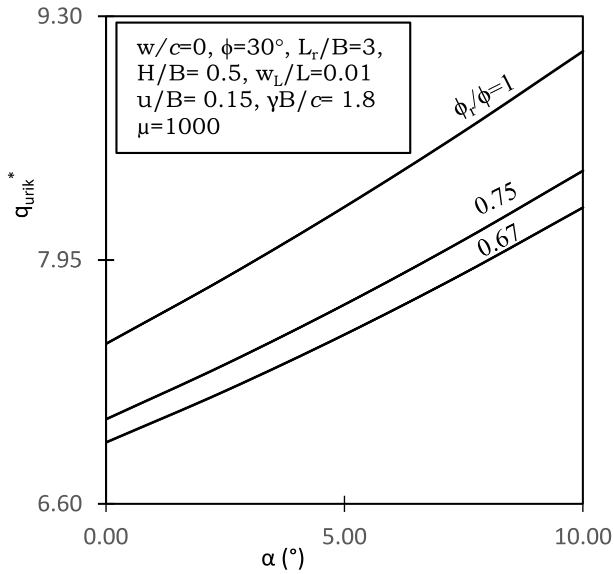

Fig. 10 : q_{urik}* versus α(°) Effect of angle interface shear resistance

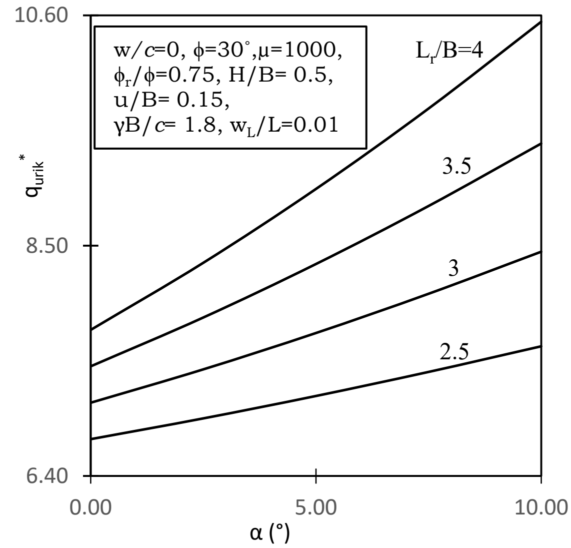

Fig. 11 : Variation of qurik* versus α -Effect of L_r/B

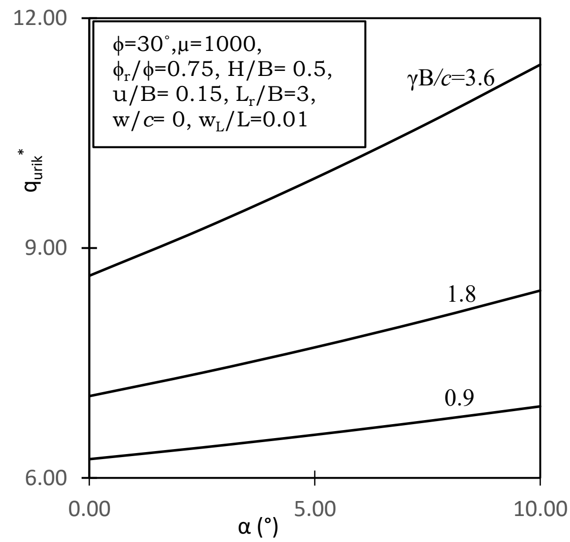

Fig. 12 : Variation of Normalised bearing capacity, q_{urik}* versus Inclination of reinforcement α -Effect of γB/c

4.6 Effect of Length of Reinforcement

Variation of normalised bearing capacity q_{urik}* with α for different various values of L_r/B for w/c=0, ϕ=30˚, H/B= 0.5, u/B= 0.15, γB/c= 1.8, μ=1000, ϕ_r/ϕ=0.75 and wL/L=0.01 are depicted in Fig.11. q_{urik}* increases from 7.07to 8.44 an increase of 19.4% with an increase in α from 0 to 10° due to combined effect of overburden stress acting on reinforcement and bond resistance mobilised due to normal stress acting on reinforcement. For an incli-nation of 5°, q_{urik}* increases from 7.13 to 9.02 an increase of 26.5% due to mobilization of bond resistance on both sides of effective length of reinforcement.

4.7 Effect of Density Gradient of Soil Bed

Variation of normalised bearing capacity, q_{urik}* with inclination of reinforcement, α for w/c=0, ϕ=30˚, H/B= 0.5, u/B= 0.15, μ=1000, ϕ_r/ϕ=0.75, L_r/B=3 and w_L/L=0.01 for different values of γB/c are depicted in Fig.12

q_{urik}* increases non-linearly from 7.07 to 8.44 an increase of 19.4% with an increase in α from 0° to 10° for γB/c=1.8 due to combined effect of overburden pressure acting on reinforcement and bond resistance mobilised due to normal stress acting on reinforcement. At 5°inclination of reinforcement, q_{urik}* increases from 6.56 to 9.91 an increase of 51% with increase in γB/c from 0.9 to 3.6 due to denser soil bed and /or wider footing with less cohesion.

4.8 Effect of Depth of Embedment

Variation of normalised bearing capacity q_{urik}* with angle of inclination of reinforcement α for w/c=0, ϕ=30˚, H/B=0.5, γB/c=1.8, μ=1000, ϕ_r/ϕ=0.75, Lr/B=3 and wL/L=0.01 for different values of u/B are shown in Fig.13.

q_{urik}* increases non-linearly from 7.07 to 8.44 an increase of 19.4% with an increase in α from 0° to 10° for γB/c=1.8 due to combined effect of increase in overbur-den stress acting on reinforcement and bond resistance mobilised due to normal stress acting on reinforcement. At 5°inclination of reinforcement, q_{urik}* increases from 7.45 to 7.96 an increase of 6.84% with increase in U/B from 0.125 to 0.175 due to increase in overburden pressure tensile force develops in reinforcement which restrains the tensile strains in the soil thus increase the bond resistance of composite medium through interface bond resistance.

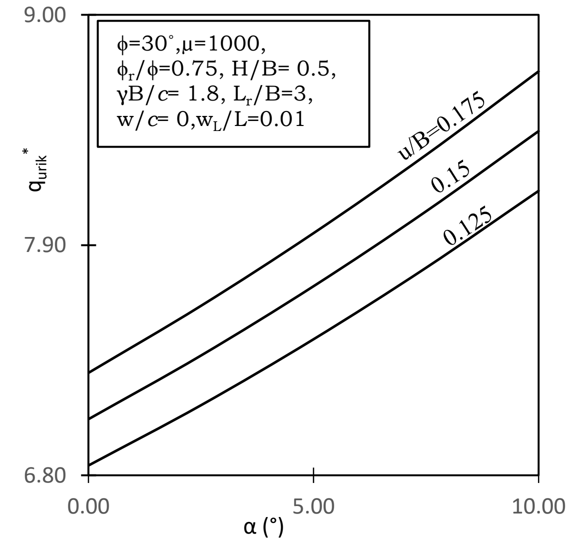

Fig. 13 : Variation of q_{urik}* versus α -Effect of u/B

4.9 Effect of Surcharge

Variation of normalised bearing capacity q_{urik}* with inclination of reinforcement, α for u/B= 0.15, ϕ=30˚, H/B= 0.5, γB/c=1.8, μ=1000, ϕ_r/ϕ=0.75, Lr/B=3 and wL/L=0.01 for various values of w/c are shown in Fig.14. q_{urik}* increases from 11.99 to 15.13 an increase of 26.2% with an increase in inclination of reinforcement from 0° to 10° for a normalised surcharge (w/c) of 1.0 due to combined effect of additional shear resistance mobi-lised due to normal stress and the increase of overburden stress exerted on reinforcement. Consideration of transverse force/displacement generates additional upward normal stress beneath reinforcement

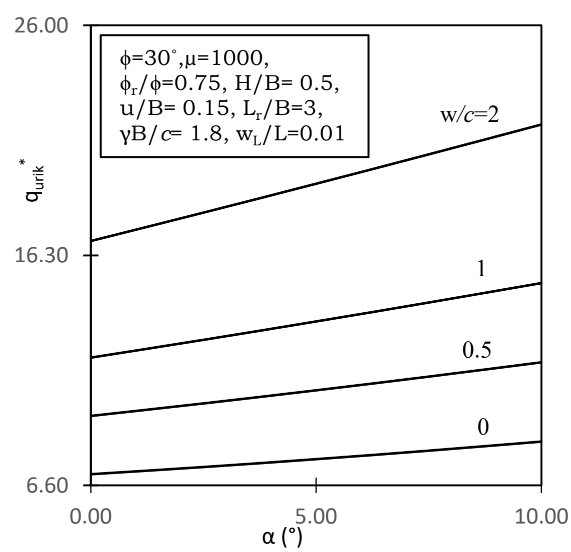

Fig. 14 : qurik* versus α (°)-Effect of w/c

and leads to generation of additional bond resistance. q_{urik}* increases from 7.70 to 19.32 an increase of 251% with increase in w/c from 0 to 2 for α=5° due to increase in normal stress act-ing on reinforcement, tensile force developed in it and re-strains the strains developed in soil thus increase the shear resistance of composite medium through interface bond resistance and contributes to increase in bearing capacity.

5. CONCLUSIONS

This paper presents method of estimating the bearing capacity of CNS bed reinforced with inclined reinforcement overlying homogeneous clay layer incorporating the kinematics of failure. Punching shear failure mode proposed by Meyerhof (1974) for thin dense sand bed overlying clay is extended to include the effects of inclined reinforcement. For the additional shear resistance mobilised in the inclined reinforcement due to transverse force/displacement theory proposed by Umashankar and Madhav (2003) is extended. Additional bond resistance mobilised in the inclined reinforcement due to normal stress acting on the reinforcement and transverse force/displacement contributes additional bond resistance beneath the reinforcement-soil-interface due to upward normal force acting on reinforcement. Thus, the bearing capacity of the footing on CNS soil bed reinforced with inclined reinforcement overlying clay layer is the sum of bearing capacity of clay layer, shear resistance mobilised in the soil bed, axial resistance mobilised in the inclined reinforcement and additional bond resistance mobilised due to transverse pull. Normalised bearing capacity factor which includes above mechanics and different bearing capacity ratios are defined and calculated for different cases and compared for different normalised displacements. Significant improvement in bearing capacity is observed over the horizontally reinforced system due to mobilization of bond resistance due to normal stress acting on inclined reinforcement and mobilization of additional shear resistance beneath the reinforcement due to consideration of kinematics of failure. (i.e. transverse displacement of reinforcement).

- For the parameters considered in the analysis, normalised bearing capacity, q_{urik}* of CNS soil bed reinforced with inclined reinforcement considering the effect of kinematics. q_{urik}* of inclined reinforcement increases significantly compared with that for horizontally reinforcement in soil bed on clay considering effect of kinematics. It increases non-linearly by 4.24%, 8.90%, 14%,19.4%for inclination of reinforcement of 2.5°,5°, 7.5°, 10° respectively. This is due to consideration of additional bond resistance mobilised due to increase in normal stress acting on the reinforcement and shear resistance mobilised along soil geotextile interface due to additional normal stress acting below the reinforcement considering the transverse displacement of reinforcement.

- q_{urik}* for a particular angle of inclination of reinforcement, α increases with μ with increase in stiffness of subgrade the transverse force required to mobilize transverse displacement increases, the reinforcement exhibits a more localised behaviour, giving rise to higher value of interface shear stresses, which ultimately leads to increase in bearing capacity.
- q_{urik}* for a particular angle of inclination of rein-forcement increases with transverse deformation be-cause of increase in upward normal stress at the inter-face. The additional bond resistance mobilised along the reinforcement caused by transverse pull improves the pull-out resistance of reinforcement
- q_{urik}* for a particular angle of inclination of rein-forcement, α increases with γB/c, ϕ, ϕ_r/ϕ, due to den-sity of soil bed/ wider footing and less cohesion, in-crease in frictional component, surface roughness of reinforcement and due to increase in normal stress tensile stress develops in reinforcement, transverse deformation causes additional normal stress to act be-neath the reinforcement due to which additional bond resistance mobilised

REFERENCES

1. Abdi, M.R., Zandieh, A.R. (2014) Experimental and numerical analysis of large-scale pull-out tests con-ducted on clays reinforced with geogrids encapsulated with coarse material. Geotextiles Geomembranes. 42(5), pp 494--504
2. Bergado, D.T., Teerawattanasuk. C., Long, P.V. (2000) Localized mobilization of reinforcement force and its direction at the vicinity of failure surface, Geotextiles Geomembranes, 18(5) pp. 311--331
3. Bonaparte, R., Christopher, B.R. (1987) Design and construction of reinforced embankments over weak foundation, Transportation Research Record No. 1153, pp. 26--39
4. Flower, J.(1982) Theoretical design considerations for fabric reinforced embankments, proceedings of 2nd International conference on Geotextiles, 3, pp 665--670
5. Gao, Y., Yang, S., Wu, Y., Li, D., Zhang, F. (2014) Evaluation of oblique pull-out resistance of rein-forcements in soil wall subjected to seismic loads. Geotextiles and Geomembranes., 42(5), pp. 515-524
6. Hariprasad, C., Uma Shankar, B. (2018) Transverse pull-out response of smooth - metal- strip Reinforce-ments Embedded in sand J. Geotech. Geoenviron. Eng., 144(3)
7. Jewel, R.A. (1992) Keynote Lecture: links between the testing, modelling and design of reinforced soil, proc. I. symposium on earth reinforcement practice, Fu Kuoka, Japan, 2, pp. 755--772
8. Kumar PSVN, Madhav, M.R. (2011) Pull-out of in-clined reinforcement in reinforced earth wall Indian Geotechnical Journal, 41 (2),pp. 95--99
9. Madhav, M.R, Manoj, T. (2004) Reinforcement - soil interactions under transverse and oblique forces. Proc., 12th Asian reginal Conference on Soil Me-chanics and Geotechnical Engineering C.F. Leung, et al.,(eds)., World Scientific, Singapore pp. 1139--1155
10. Meyerhof, C.G. & Hanna, A.M (1978) Ultimate bear-ing capacity of foundation on layered soils under in-clined load, Canadian Geotechnical Journal,15(4), pp 565-572.
11. Meyerhof, C.G.(1974) Ultimate bearing capacity of footings on sand layer overlying clay, Canadian Ge-otechnical Journal, 11 (2), pp. 223--229
12. Michalowski, R.L., Shi, L. (1985) Bearing capacity of footings over two-layer foundations soil Journal of geotechnical Engineering 16 (12), pp. 1902--1906
13. Narasimha Reddy, G.V., Madhav, M.R., Saibaba Reddy, E. (2009) Kinematics and analysis of rein-forced soil wall linear backfill response, International Journal of Geotechnical Engineering, pp. 39--50
14. Patra, S., Shahu, J.T. (2012) Pasternak model for oblique pull-out of inextensible reinforcement J. Ge-otech. Geoenviron Engg., 10.1061/ (ASCE) GT, 1943-5606.0000720, pp. 1503--1513
15. Quast, P. (1983) Polyester reinforcing fabric mats for the improvement of embankment stability, Proc. Of 8th Int. conference on Soil mechanics and Foundation Engineering, 2, pp. 531--534
16. Rowe, K.R., Soderman, K.L. (1984) Comparison of predicted and observed behaviour of two test em-bankments, Geotextiles and Geomembranes, 1(2), pp. 143--160
17. Sahu, J.T. (2007) Pull-out response of inextensible sheet reinforcement subject to oblique pull. J. Ge-otech. Geo environmental Eng., 10.1061/ (ASC) 1090-0241 (2007) 133;11(1440), pp. 1440--1448
18. Sahu, J.T., Hayashi, S. (2009) Analysis of extensible reinforcement subject to oblique pull. J. Geotech Ge-oenviron. Engg., 10.1061/ (ASCE) GT, 1943-5606.0000019
19. Sobhi, S., Wu. (1996) An interface pull-out formula for extensible sheet reinforcement. Geosynthetic International, 3(5), pp. 565--582
20. Uma Shankar, B., Madhav, M.R. (2003) Analysis of inextensible sheet reinforcement subjected to trans-verse displacement/force Linear subgrade response, Geotextiles and Geomembranes, 21(2), pp. 69--84

REVIEW OF CHARACTERIZATION OF GROUND GRANULATED BLAST SLAG (GGBS) AS GEOMATERIAL

Satyajit Roy[1], Vikas Kumar Jain[1], Manish Gupta[1] and R Chitra[1]

ABSTRACT

Ground granulated blast slag (GGBS) is the granular by-product produced by steel manufacturing processes. Industrial granular solid waste materials like fly-ash, red mud and slag can be engineered chemically or mechanically to achieve desirable properties as geo-materials (Karol 2003). These engineered geo-materials have a huge range of geotechnical applications such as ground improvement materials, landfill materials for highway and railway embankment, as land fill liners at engineered waste disposal facilities and as stabilizing agent for natural slopes. It can also be used in construction of tailling dam which is used to store by-products of mining operation. There have been number of studies/ cases like soft soil stabilization using ground granulated blast furnace slag, characteristics of core materials mix of GGBS with locally available soil used in slime dam/tailing dam construction, soil stabilization using ground granulated blast furnace Slag, use of GGBS as an alternative to natural sand etc. From these studies, investigators concluded that use of GGBS results in improvement of physical and strength properties of soil.

GGBS is of silty type materials having silt content around 15-20%. GGBS is non plastic having liquid limit around 30 to 33%.Maximum dry density (MDD) and optimum moisture content of GGBS varies from 12 g/cc to 16 g/cc and 21% to 26% respectively. As per IS 16714 - 2018, the minimum fineness should be 320 m²/kg. The main chemical constituents of GGBS are CaO, SiO_2, Al_2O_3, Fe_2O_3 etc.

It has been reported that with the increase of GGBS content specific gravity increases whereas Liquid limit, plastic limit, shrinkage limit and plasticity index decreases. Hydraulic conductivity of Brahamaputra river sand found to be decreases with addition of GGBS. Studies also indicate that unconfined compressive strength also increases in general. GGBS have been used in stabilization of black cotton soil, soft soil etc. If other engineering properties like consolidation, shear strength, in presence of different percentage of GGBS can be studied, than it will be easier to declare it as Geomaterial.

1. INTRODUCTION

Ground Granulated Blast furnace Slag (GGBS) is a byproduct from the blast furnaces used to make iron. These operate at a temperature of about 1500 degrees centigrade and are fed with a carefully controlled mixture of iron ore, coke and limestone. The iron ore is reduced to iron and the remaining materials form a slag that floats on top of the iron. This slag is periodically tapped off as a molten liquid and if it is to be used for the manufacture of GGBS it has to be rapidly quenched in large volumes of water. The quenching optimises the cementitious properties and produces granules similar to coarse sand. This granulated slag is then dried and ground to a fine powder. Fig. 1 represents sources of Ground Granulated Blast Slag (GGBS) and Fig. 2 shows sample of GGBS.

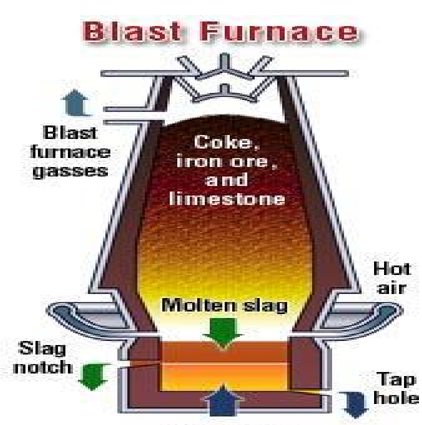

Fig 1 : Sources of Ground Granulated Blast Slag (GGBS)

1. Central Soil and Materials Research Station, New Delhi

Fig. 2 : Sample of GGBS

The steel consumption per capita in India is 61 kg which is much lower when compared to global average of 208kg.National Steel Policy (India), 2017 aims the steel production to grow per capita steel consumption 160 kg by 2030. This policy also aims to increase the steel production in India to 300 million tons by 2030 compared to current production rate of 95.6 million tons. Eventually, this will lead to an inevitable large quantity of steel slag production.

Therefore, an efficient method of utilization of slag is necessary for sustainable development. Geotechnical applications of granular industrial waste materials provide opportunity to utilize large quantity of industrial granular by-products as geo-materials. However, the geo-sphere and its environment should be considered as categorically sensitive as it is also in contact with groundwater.

In this study, attempt has been made to analyse/study the various geotechnical properties of GGBS for its classification as geo-material.

2. CHEMICAL COMPOSITION OF GROUND GRANULATED BLAST FURNACE SLAG (GGBS)

Table 1 reprsents Chemical composition (w/w %) of slag (Obtained from TATA Steel, Jamshedpur, Dubey A A et. al (2018))

The most abundant mineral phase identified qualitatively was Portlandite[$Ca(OH)_2$]; this is expected because EAF steel slag contains 46% lime (CaO). Water converts free lime into Calcium Hydroxide [$Ca(OH)_2$]. Periclase (MgO), Calcite ($CaCO_3$) are also identified as major phases.

3. COMPARISON OF GGBS WITH OTHER INDUSTRIAL WASTE PRODUCT

Soil stabilization is a technique used to change different soil properties and to enhance its performance for engineering purpose. Admixture may be chemical binder, industrial waste (GGBS, Rice Husk etc), cement and fly ash. The table No. 2, showing comparison of Chemical properties of Cement clinker, Fly ash an Rice Husk with GGBS (Shetty M.S.(2012) "Concrete Technology").

Table 1 : Chemical composition of slag

Mineral	% Composition
Fe_2O_3	14.45
CaO	46.62
SiO_2	11.13
P_2O_5	2.32
MgO	5-15
MnO	0.41
Al_2O_3	1.66
TiO_2	0.75
Cr_2O_3	0.137
LOI	10.6
Na_2O	0.029
K_2O	0.008
C	1.41
S	0.19

4. CHEMICAL AND PHYSICAL REQUIREMENT OF GGBS AS PER INDIAN STANDARD

Indian Standard IS 16714:2018, "Ground Granulated Blast Furnace slag for use in cement,mortar and concrete"-specification covers chemical and physical requirement of ground granulated blast furnace slag to be used in manufacture cement and as mineral admixture in mortar and concrete making. Table No. 3 represents chemical requirement of GGBS.

Table No. 2 : Comparison of chemical properties of different industrial products (Shetty M.S. (2012) "Concrete Technology")

Sl No.	Constitute	Percentage Content			
		Cement Clinker	Blast Furnace Slag (GGBS)	Fly ash	Rice Husk
1	CaO	60.0-67.0%	30.0-45.0%	1.0-3.0%	0.5-1.0%
2	SiO_2	17.0-25.0%	30.0-38.0%	35.0-60.0%	90.0-95.0%
3	Al_2O_3	3.0-8.0%	15.0-25.0%	10.0-30.0%	0.5-1.0%
4	Fe_2O_3	0.5-6.0%	0.5-2.0%	4.0-10.0%	0.1-1.0%
5	MgO	0.1-4.0%	4.0-17.0%	0.2-5.0%	0.1-1.0%
6	MnO_2	-	1.0-5.0%		
7	Glass	-	85.0-98.0%	20.0-30.0%	
8	Specific Gravity	3.15	2.9	2.1-2.6	2.1

Table 3 : Chemical requirement of GGBS as per IS code (IS 16714:2018)

Sl. No.	Constitute/Characteristics	Percent by mass	Method of Test, Ref No.
1	Manganese oxide(MnO), Max	5.5%	IS 4032
2	Magnesium oxide (MgO), Max	17.0%	IS 4032
3	Sulphide sulphur (S), Max	2.0 %	IS 4032
4	Sulphate(as SO3), Max	3.0 %	IS 4032
5	Insoluble residue, Max	3.0%	IS 4032
6	Chloride content,Max	0.1%	IS 4032
7	Loss on ignition, Max	3.0 %	IS 4032
8	CaO+MgO+1/3 AlO_3,Min SiO_2 +2/3 AlO_3	1.0%	IS 4032
9	CaO+MgO+Al_2O_3, Min SiO2	1.0 %	IS 4032
10	CaO+CaS+1/2MgO+ Al_2O_3, Min SiO2 +MnO	1.5%	IS 4032

Moreover, the moisture content of GGBS, when tested as per IS 16714:2018 (Annex B), shall not exceed 1%.The glass content of GGBS shall not be less than 85% when determined by the method of optical microscope given in IS 16714:2018 (Annex C).

GGBS shall comply with the physical requirement given in table No.4:

Table No. 4 : Physical requirement of GGBS as per IS code (IS 16714: 2018)

Sl No.	Constituent	Requirement	Method of Test
1	Fineness, m^2/kg,Min	320	IS 4031(Part 2)
2	Slag activity index (a) 7 days (b) 28 days	 Not less than 60% of control OPC 43 Grade cement mortar cube. Not less than 60% of control OPC 43 Grdae cement mortar cube.	

Slag activity index (SAI) shall be determined using blend of 50% GGBS and 50% control OPC 43 conforming to IS 269,having total alkalies (Na_2O+0.658K_2O) not less than 0.6% and more than 0.9%).The blend shall be tested in accordance with IS 4031(Part 6), for determining compressive strength of mortar.

SAI shall be determined as:

$$\frac{\text{compressive strength of the mortar cube using blend}}{\text{compressive strength of control OPC using blend}} \times 100$$

5. PHYSICAL PROPERTIES OF GGBS

The criteria which are relevant for classifying soil/ admixtures for engineering purposes are: (i) size of particles (ii) stickiness or plasticity of soil.

5.1 Grain Size Analysis & Atterberg Limits

(a) Dubey A A et.al. (2018) studied classification of GGBS (Slag from Tata Steel, Jamshedpur), and found relatively well graded and contains 17.35% silt. Therefore it classified as SM as per USCS with Cu = 6 and Cc= 1.27.The Figure 3, represents gain size distribution curve for Brahamputra sand and fresh steel slag

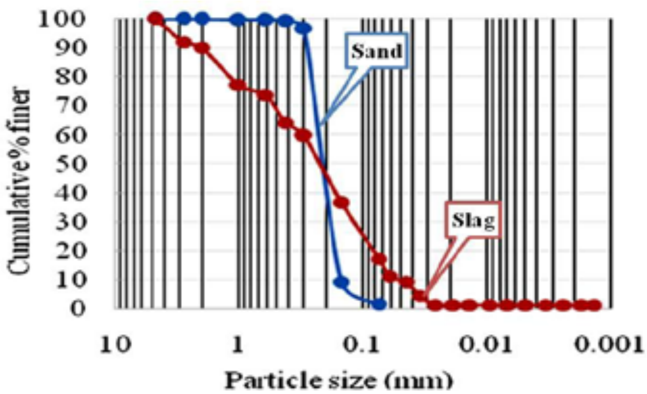

Fig. 3 : Grain-size distribution curves for Brahmaputra sand and fresh steel slag (Dubey A A et.al. 2018)

(b) Sharma & Sivapullaiah, (2011), studied the Atterberg limits of GGBS and shown in tabular form in table No. 5:

Table No. 5 : Physical properties of GGBS, (Sharma & Sivapullaiah, 2011)

Properties	BC soil	Fly ash	GGBS
Specific gravity	2.61	2.01	2.83
Liquid limit : %	76	31.34	31.5
Plastic limit : %	35	NP	NP
Plasticity index : %	41	NP	NP
Shrinkage limit: %	10	NP	NP
Modified Free swell index : cm³/g	4.22	0	0
OMC:%	33	22	26
MDD (kN/m³)	13.56	12.83	12/74

5.2 Specific Gravity

(a) Sharma & Sivapullaiah, (2011), studied the specific gravity of GGBS and found value as 2.83.

5.3 Relative density

(a) Dubey A A et.al. (2018) studied relative density of GGBS,Maximum dry unit weight ((γ_{max}) and minimum dry unit weight (γ_{min})) for steel slag were observed as 16.072 kN/m^3 and 20.057 kN/m^3.

5.4 Free Swell Index:

(a) Dubey A A et. (2018) studied et. al. studied free swell index of GGBS. Short tome free swell index of GGBS shown in table No. 6

Table No. 6 : Short Time Free Swell Index (Dubey A A et. 2018)

Sample No	Sample analysed after	Free swell Index
1	24 hr	0.0
2	7 days	3.85
3	28 days	3.85

5.5 pH

(a) Dubey A A et. (2018) studied that during the slag-water interaction, it was observed that the slag changes the pH of distilled water (initial pH =6.8) drastically (final pH= 12). This study suggests that steel slag is a heavy, highly alkaline and calcium rich industrial waste.

6. SOIL STABILIZATION

Some important work reported in literature on GGBS:

(a) Sharma & Sivapullaiah, (2011) studied the use of fly ash and/ or GGBS with lime as a stabiliser added to a black cotton soil.

(i) The research presents stabilization of BC soil with GGBS and enhancing the cementituos properties of Fly ash with GGBS. The figure No.4 presents effects of dry density and OMC in GGBS-soil mixture.

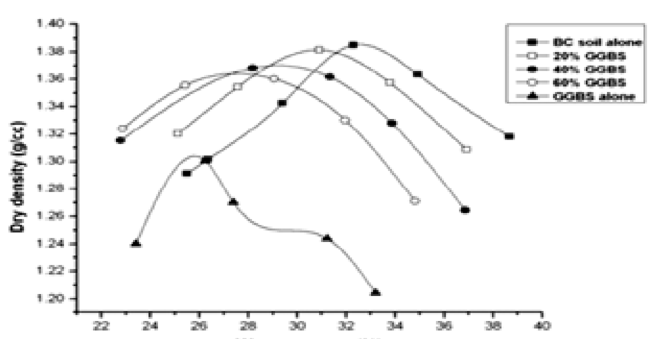

GGBS-Soil Mixture	OMC (%)	MDD (gm/cc)
BC soil alone	33.00	1.386
20% GGBS	31.00	1.382
40% GGBS	29.00	1.370
60% GGBS	27.50	1.364
GGBS alone	26.00	1.316

Fig. 4 : Effets of dry density and OMC in GGBS-soil mixture. (Sharma & Sivapullaiah, 2011)

It is interesting to note that both OMC and MDD decrease with increase in the GGBS content. Generally addition of silt or sand or fly ash to fine grained soil decreases OMC and increases MDD.

The decrease in OMC is obviously due to the addition of GGBS which is relatively coarser relative to BC soil.Addition of coarser particles reduces the water holding capacity due to the reduction of the clay content. The decrease in MDD, in spite of increase in OMC, is due to the predominant effect of high frictional resistance offered by relatively coarser GGBS due to size and surface texture resisting the compactive effort effectively.

(ii) The variation of the unconfined compressive strength test with GGBS content for different curing periods has been shown in the Fig 5.

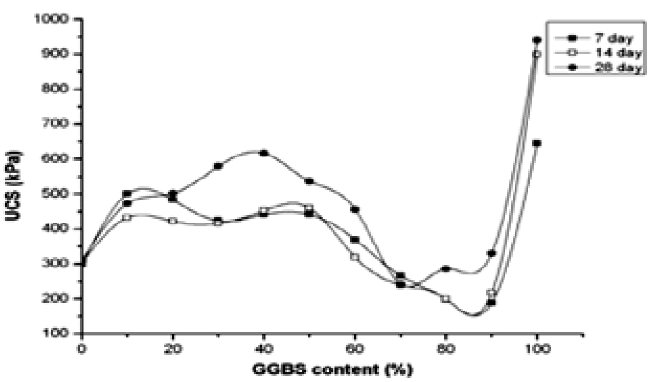

Fig. 5 : Unconfined compressive strength test with GGBS content for different curing period (Sharma & Sivapullaiah, 2011)

From the figure it can be seen that the unconfined compressive strength (UCS) of BC soil increases with the addition of small amount of about GGBS which remains constant up about 40% addition of GGBS.With further addition of GGBS the UCS decreases continuously and reaches lowest value with the addition of 90% of GGBS.

(iii) The variation of UCS of Fly ash with different GGBS content but without lime is shown in Fig. 6.

It can be seen from the figure that the gain in strength of the Fly ash-GGBS mixtures is extremely good for the 7 day curing period. The strength increased from 62 kPa to 540 kPa with addition of 50% of GGBS. The relationship found between the unconfined compressive strength of the Fly ash with GGBS content is linear with a discontinuity in between 20 to 30% of the GGBS content. The discontinuity may be due to the

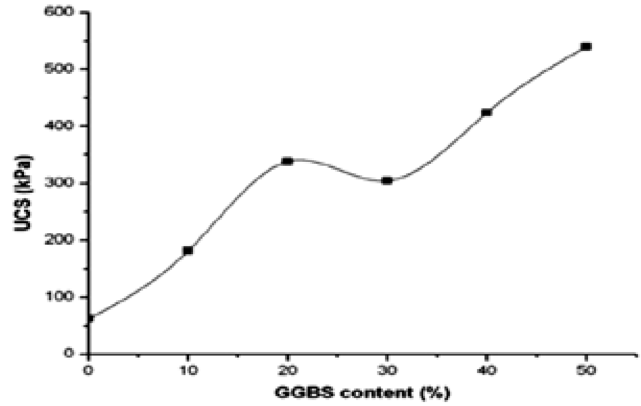

Fig. 6 : Variation of UCS of Fly ash with GGBS content (Sharma & Sivapullaiah, 2011)

disturbance caused to development of soil matrix and also by unfavourable gradation of Fly ash-GGBS mixtures.

(iv) Fig 7. shows the variation of UCS of Fly ash with different percentages of GGBS at lime content of 2 and 4 % for 7day curing period.

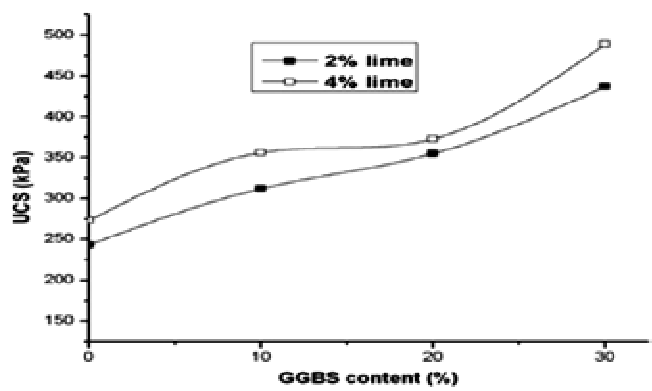

Fig. 7 : Variation of UCS of Fly ash with GGBS content along with lime, (Sharma & Sivapullaiah, 2011)

It can be seen from the figure that with the addition of lime has further improved the UCS of the Fly ash GGBS mixtures. One interesting point can be noticed from this figure that the discontinuity which occurs in the variation of UCS strength with GGBS content (between 20% and 30% GGBS content without lime is eliminated with the addition of lime. It means the disturbance is balanced by the formation of further pozzolanic compounds in the presence of lime. Further the strength achieved is higher at still lower GGBS content. The relationship between the strength variations of Fly ash-GGBS mixtures is almost linear.

Increase in strength of Fly ash with addition of GGBS can be explained with two reasons:

Firstly, the formation of compounds (C-S-H gel) possessing cementing properties in the presence of highly reactive siliceous and aluminous materials and water and secondly addition of GGBS to Fly ash makes the mix well graded which in turn increases the compacted density and hence the mechanical strength of the compacted mixture.

(b) Yadu & Tripathi, (2013) investigated the potential of using GGBS as a stabiliser for the soft soil. GGBS used in the study was blended with soft soil in different proportions i.e. 3, 6, 9 & 12 % by weight of soft soil to obtain optimum amount for stabilization. The Fig. No. 8 represents physical and strength properties of soft soil mixed with GGBS at various percentage:

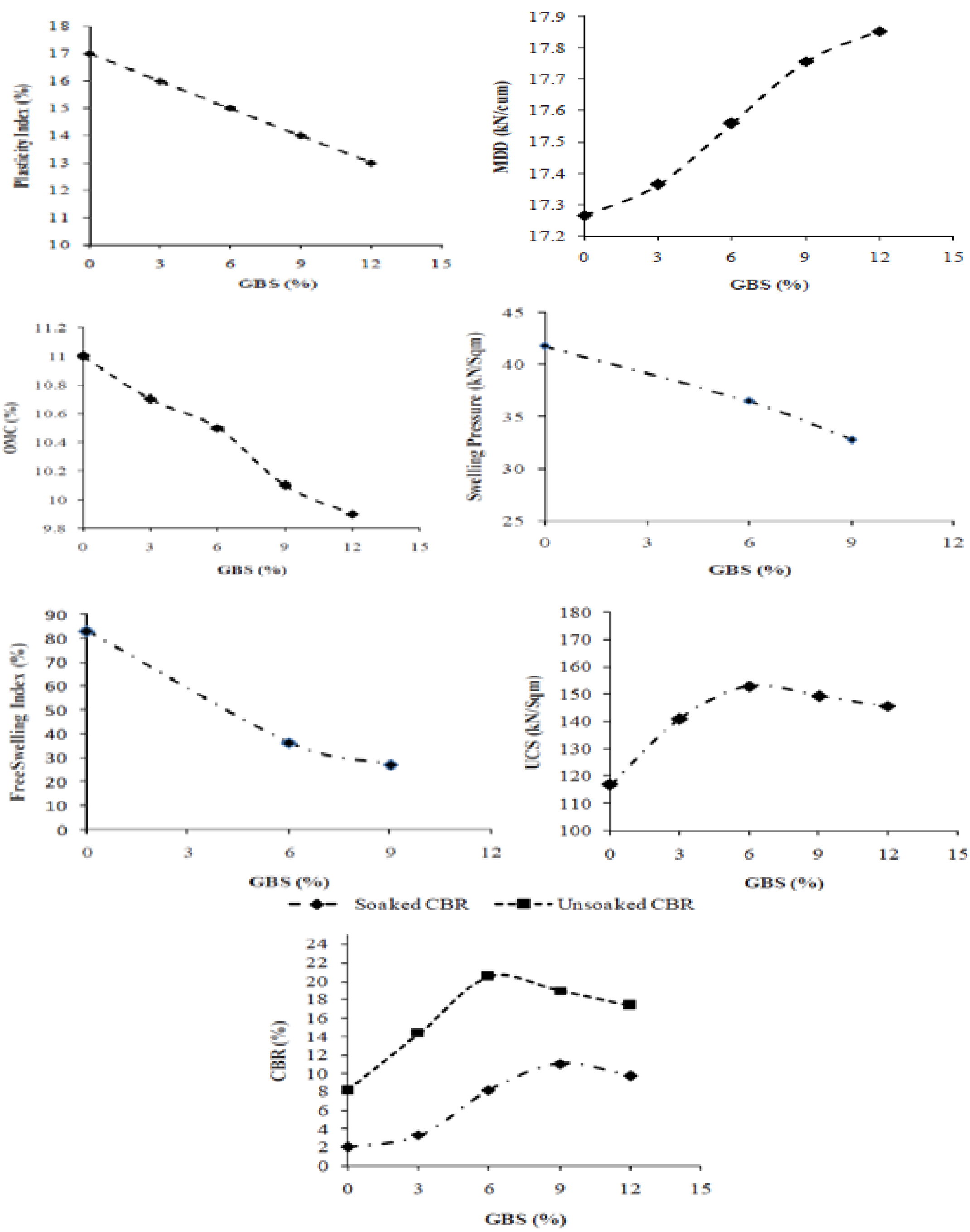

Fig. No. 8 : Comparison of physical and strength properties of soft soil mixed GGBS (Yadu & Tripathi, (2013) The result indicates that the use of GGBS significantly improves the physical and strength properties of soil. MDD increased while OMC decreased with addition of GGBS to the soft soil. There is significant reduction in the swelling behavior of the soil. Based on the strength test, optimum amount of GGBS was determined as 9%. Soaked CBR and UCS values increased about 400% and 28% respectively by the addition of optimum amount of GGBS. Moreover blended mix of 9% GGBS reduces the free swelling index and swelling pressure of about 67% and 21% respectively from its unstabilised counterpart.

(c) Ormila & Preethi, (2014) studied the effect of adding GGBS to expensive soil collected from Palur, Tamil Nadu at various percentages (15%, 20%, and 25%). In the study, the soil sample was mixed with different percentages of flyash (5, 10%, 15% and 20%) and GGBS (15%, 20%, and 25%) to find the variation in its original strength. The fig. No. 9(a,b,c) represents UCS values for different percentage of GGBS by curing for 21, 7 & 14 days.

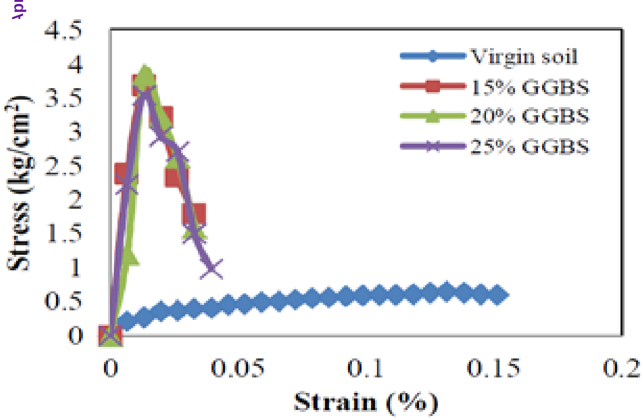

Fig. 9(a) : UCS value for different % of GGBS curing for 21 days (Ormila & Preethi, 2014)

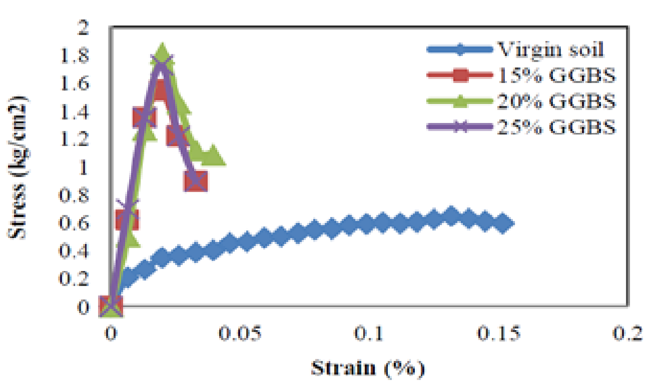

Fig. 9(b) : UCS value for different % of GGBS by curing for 7 days(Ormila & Preethi,2014)

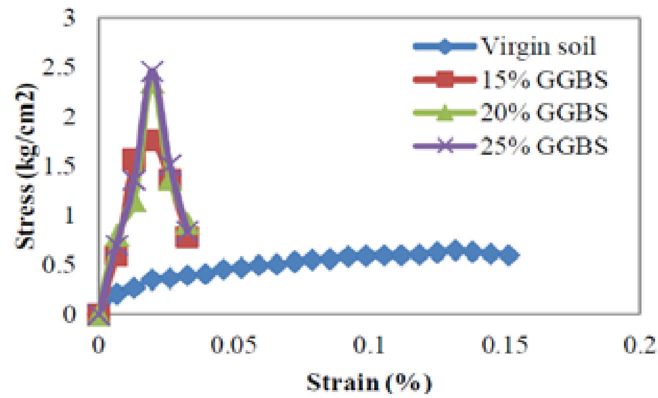

Fig 9(c) : UCS value for different % of GGBS curing for 14 days (Ormila & Preethi,2014)

They indicated that addition of GGBS can improve the unconfined compressive strength of the soil given that 20% GGBS is the optimum content with an increase in strength of 73.79% after curing of 21 days.

7. CONCLUSIONS

(a) GGBS is granular by product of steel industry. It is silty type material, grey in colour, having glass content not less than 85%. Due to its high glass content, it should handle with care.

(b) There are similarity between GGBS and ordinary Portland cement in oxides types but not the percentage (Sha and Pereira, 2001; Oner and Akyuz, 2007). During the production of GGBS, its cementitious characteristics increases because molten slag chills rapidly after leaving the furnace. The rapid chilling leads to decrease in the crystallisation and transforms the molten slag into a glassy material (Thanaya, 2012). W.A Tasong et al. (1999)studied the chemical composition of GGBS by using X-Ray diffractometry technique and electron microscopy. He deduced that GGBFS comprises mainly of CaO, SiO2, Al2O3 and MgO.

(c) With the increase of GGBS contents in soil, the specific gravity values of the Soil-GGBS mix increase due to GGBS particles having higher specific gravity than soil particles.

(d) As GGBS is of silty type materials(non plastic) having silt content around 15-20%, so the liquid limit (LL), plastic limit(PL), Shrinkage Index (SI), and plasticity index (PI) decreases of soil mixed with GGBS decreases.

(e) With the increase of % GGBS in soil, Unconfined Compressive Strength value increases.

(f) Free swell index value of GGBS is 0 after 24 hour of observation. However after 7 & 28 days it comes out as 3.85.

(g) GGBS are being used for stabilizing of problematic soil like soft soil, black cotton soil etc. which is also beneficial to the environment because if dumped as waste, these materials can cause severe hazards to the nearby land and environment.

(h) These materials are abundantly available in every country and can be used as a partial replacement of cement as production of cement is a major cause for CO2 and other greenhouse gas emission.

(i) The high alkalinity of slag, make raw GGBS dangerous for aquatic life. However, the high alkalinity of slag may be used for treatment of acidic soil. The high concentration of calcium may be utilized in cementation processes.

(j) GGBS can used in the Slime Dam / Tailing dam (both are same) construction, as studied by Chakraborty U B (2019). The Syncrude Mildred Lake Tailings Dyke in Alberta, Canada, is an embankment dam about 18 kilometers long and from 40 to 88 metres high. It is the largest dam structure on earth by volume, and as of 2001 it was believed to be the largest earth structure in the world by volume of fill. There are key differences between tailings dams and the more familiar hydroelectric dams. Fig. 10(a)&(b) shows Tailings Dam, West Cornwall, England and Slime dam Joda Iron Mine, Jamshedpur, India.

(k) If other engineering properties like consolidation, shear strength, dispersivity, hydraulic conductivity (clay) at presence of different percentage of GGBS can be studied, than it will be easier to declare it as Geomaterial.

Fig. 10(a) : Tailings Dam, West Cornwall, England Slime dam Joda Iron Mine, Jamshedpur, India

Fig. 10(b) : Slime dam Joda Iron Mine, Jamshedpur, India

(I) However, the application of any industrial waste to geotechnical system must be considered a sensitive issue as most of the geotechnical systems are in the vicinity of ground water. Any toxic element leaching can contaminate the ground water source leading to adversity.

REFERENCES

1. Indian Standard Code, IS 16714 -2018: Ground Granulated Blast Furnace Slag for use in cement, mortar and concrete-Specification. Indian Standard Code, Bureau of Indian Standard.
2. Indian Standard Code, IS 2720(Part 4)-1985 Grain size analysis, Methods of test for soil, Indian Standard Code, Bureau of Indian Standard.
3. Indian Standard Code, IS 2720(Part 5)-1985 Determination of Liquid limit and plastic limit, Methods of test for soil, Indian Standard Code, Bureau of Indian Standard.
4. IS 2720 (Part 3/Sec 2)-1980, Determination of specific gravity of fine, medium & coarse grained soil. Methods of test for soil, Indian Standard Code Bureau of Indian Standard.
5. IS 2720 (Part 14)-1983, Determination of density index (relative density) of cohesionless soil Methods of test for soil, Indian Standard Code Bureau of Indian Standard.
6. IS 2720 (Part 15)-1986, Determination of consolidation properties, Methods of test for soil, Indian Standard Code Bureau of Indian Standard.
7. IS 2720 (Part 7)-1980, Determination of water content-dry density relation using light compaction, Indian Standard Code Bureau of Indian Standard.
8. IS 2720(Part 17)-1986, Determination of Permeability, Methods of test for soil, Indian Standard Code, Bureau of Indian Standard.Bureau of Indian Standard.
9. IS 2720(Part 12)-1981, Determination of Shear strength parameter of soil from consolidated undrained triaxial compression test with measurement of pore water pressure , Indian Standard Code, Bureau of Indian Standard.Bureau of Indian Standard.
10. IS: 2720(Part 40)-1977, Determination of Swell Index, Methods of test for soil, Indian Standard Code, Bureau of Indian Standard.
11. IS: 2720(Part 10)-1973, Determination of unconfined compressive strength, Indian Standard Code, Bureau of Indian Standard.
12. Shetty M.S.(2012) „Concrete Technology"
13. Ormila.T.R & Preethi.T.V. (2014). Effect of Stabilization Using Fly ash and GGBS in Soil Characteristics. International Journal of Engineering Trends and Technology (IJETT), V. 11 (6), pp 284- 289.
14. ONER, A. & AKYUZ, S. 2007. An experimental study on optimum usage of GGBS for the compressive strength of concrete. Cement and Concrete Composites, 29, 505-514.
15. Sharma. A.K & Sivapullaiah, P.V. (2011). Soil stabilisation with waste materials based binder. Proceedings of Indian Geotechnical Conference. Kochi India. 15-17 December, V 119 pp.413-416.
16. Shi, C. (2001). Studies on Several Factors Affecting Hydration and Properties of Lime-Pozzolan Cements. J. Mater. Civ. Eng., 13(6), pp.441-445.
17. Yadu. L & Tripathi. R.K. (2013) Stabilization of Soft Soil with Granulated Blast Furnace Slag and Fly Ash, International Journal of Research in Engineering and Technology, Volume: 02 Issue: 02.
18. Chakraborty U B (2019) "Characteristics of Core Materials Mix of GGBS with Locally Available Soil Used in Slime Dam Construction at Joda Iron Mines."Electronic Journal of Geotechnical Engineering, 2019(24.01), pp 199-210.
19. Dubey A A et.(2018)(IGC -2018) " Characterization of Steel Slag as geomaterial"

COMPRESSIBILITY OF POLYPROPYLENE FIBRE REINFORCED FINE SAND

C. N. V. Satyanarayana Reddy[1], D. Jyothi Swarup[2] and M.R. Aparna[3]

ABSTRACT

Fibre reinforced soils are gaining applications in civil engineering constructions due to improved engineering benefits of increased friction, permeability and shear strength. Particularly stabilization of granular materials with randomly distributed fibres has received much attention due to ease in mixing and placement. Though many studies are reported on improved angle of shearing resistance of fibre reinforced soils, studies on compressibility of synthetic fibre reinforced soils are limited. Hence, the present study is carried out to evaluate the compressibility of polypropylene fibre reinforced fine sand for fibres of 6mm and 12mm length in proportions of 0.5, 1.0 and 1.5% by weight. The compression indices of the fibre reinforced soils are determined from consolidation tests performed in oedometer. The study revealed that 12mm fibre reinforced sand has lesser compressibility over 6mm fibre reinforced sand at a given fibre content and the compressibility of sand stabilized with fibre of content of 1.5% (by weight) has resulted in compressibility less than that of low compressible clays.

Keywords *: Fiber Reinforced Fine Sand, Compressibility, Coefficient of Consolidation, Compression Index.*

1. INTRODUCTION

Soil is widely used as construction material in various Civil engineering structures such as embankments, Reinforced Earth Retaining Walls (RERW), backfill material in basements of buildings, retaining wall backfills and trenches. Over the last two to three decades, several waste materials such as crusher dust, coal ashes which include Fly ash, Pond ash and Bottom ash are being used as fill or backfill material. Also, fibre reinforced soils are being considered to replace the conventional fill/ backfill materials to overcome scarcity of the materials and to reduce the costs of projects.

Over the last two decades, the engineering benefits of soils with randomly oriented fibres are studied by various researchers. The effect of fibre addition is reported to increase the angle of shearing resistance of granular sols (Yetimoglu and Salbas 2003; Venkatappa Rao et. al. 2005; Satyanarayana Reddy and Sireesha, 2014). The optimum fibre content is reported to be 1%-1.5% by weight for stabilization of sand. Hesham et al. (2016) have reported that dry loose fiber-reinforced sand achieves the same shear strength of heavily compacted unreinforced moist sand. In clays, the effect of randomly distributed fibre is reported to have increased permeability of soil and improve strength characteristics (Kumar and Tabor 2003; Mariamma Joseph 2011). Addition of Fibres of varying length has indicated reduced swell pressures of expansive clays (Viswanadham et al. 2009; Sireesha and Satyanarayana Reddy, 2018).

As steel fibres get corroded, synthetic fibres are preferred to stabilize the soils. Polypropylene and polyester fibres have been used by the researchers due to their better durability and particularly better resistance to water. Though the researchers have studied the effect of randomly oriented fibres in soils on compaction characteristics, Permeability and strength characteristics, compressibility is not studied. It is essential to have the compressibility characteristics of fibre reinforced soil before considering it as fill material in construction of Reinforced Soil retaining walls and as backfill material behind retaining walls.

Recent studies have indicated the potential for use of fibre reinforced fine sand as fill material in construction of Embankments and Retaining walls. So, in the present study, the compressibility characteristics of fine sand reinforced with polypropylene fiber of 6mm and 12mm lengths with fiber contents of 0.5%, 1.0% and 1.5% (by weight) are studied.

2. MATERIAL PROPERTIES

Fine sand used in the study is procured from Visakhapatnam beach, India. The properties of fine sand determined from laboratory investigations are presented in Table 1.

Polypropylene fibres of 6mm and 12mm length supplied by Reliance Industries Limited are used in the present study. From Scanning electron microscopy, the cross section of fibre is observed to be triangular and diameter of fibre is measured to be 35-40 microns.

1. Professor, Department of Civil Engineering, College of Engineering, Andhra University,Visakhapatnam

2. Research Scholar, Department of Civil Engineering, College of Engineering, Andhra University, Visakhapatnam

3. Formerly Postgraduate Student, Dept. of Civil Engineering, College of Engineering, Andhra University, Visakhapatnam

Table 1 : Engineering properties of Fine Sand

Property	Value
Specific Gravity	2.66
Grain Size Distribution	
(i) Gravel (%)	0
(ii) Sand (%)	95
(a) Coarse Sand	0
(b) Medium Sand	26
(c) Fine Sand	70
(iii) Fines (%)	04
(iv) Uniformity coefficient, Cu	2.0
(v) Coefficient of curvature, Cc	0.8
Plasticity Characteristics	
(i) Liquid Limit (%)	NP
(ii) Plastic Limit (%)	NP
IS Classification	SP
Compaction Characteristics	
(i) Optimum Moisture Content (%)	12.0
(ii) Maximum Dry Density (g/cc)	1.76

3. COMPACTION CHARACTERISTICS OF FIBRE REINFORCED FINE SAND

The compaction characteristics of fine sand mixed with 6mm and 12mm length polypropylene fibers in varying proportions are determined from IS heavy (modified proctor) compaction tests (IS 2720 part 8, 1993). The compaction characteristics of fibre reinforced fine sand are presented in Table 2.

Table 2 . Compaction characteristics of fiber reinforced fine sand

Fiber Length	Compaction Characteristics	Fiber Content		
		0.5%	1.5%	1.0%
6 mm	OMC (%)	13.8	15.6	17.5
	MDD (g/cc)	1.73	1.63	1.56
12 mm	OMC (%)	13.2	15.4	16.2
	MDD (g/cc)	1.75	1.68	1.59

The results presented in Table 2 indicate that the MDD values of fibre reinforced fine sand decrease with increase in fibre content for both 6mm and 12mm length fibres. However, at a given fibre content, the compacted MDD of 12mm fibre reinforced sand exhibited slightly higher value than 6mm fibre reinforced sand. OMC values of fibre reinforced sand are observed to be higher for 6mm fibre over 12mm fibre, which can be attributed to higher specific surface of 6mm fibre compared to 12mm fibre at a given fibre content (by weight). The higher MDD values of 12mm fibre reinforced sand are due to better workability and interaction of 12mm fibre over 6mm fibre.

4. COMPRESSIBILITY STUDIES ON FIBRE REINFORCED FINE SAND

The compressibility of fibre reinforced fine sand is determined by performing consolidation tests as per IS 2720 part 15 (1963) on specimens of 60mm diameter and 20mm thick prepared at OMC and MDD in oedometer. The specimens are subjected to loading of 5 kN/m^2, 10 kN/m^2, 20 kN/m^2, 40 kN/m^2, 80 kN/m^2, 160 kN/m^2, 320 kN/m^2 and 640 kN/m^2 and the equilibrium void ratios of the specimens are determined under applied loads by height of solids method. Compressibility of fine sand and fibre reinforced fine sand are evaluated in terms of compression indices. Compression index is determined as slope of virgin compression curve of void ratio-effective stress plot. The results of consolidation tests are presented in Table 3.

Table 3 : Compression index of fibre rinforced fine sand

Fibre length (mm)	Fibre content (%)	Compression index	
		OMC-MDD state	Saturated state
0	0	0.033	0.037
6	0.5	0.039	0.043
6	1.0	0.056	0.066
6	1.5	0.09	0.113
12	0.5	0.041	0.045
12	1.0	0.049	0.058
12	1.5	0.068	0.085

From results presented in Table 3 and Fig. 1 and Fig. 2, The values Cc of fibre reinforced sand are observed to be about 10-25% higher in saturated condition compared to OMC-MDD state. It can be further seen that the compressibility of 6mm fibre reinforced sand is higher compared to 12mm fibre reinforced fine sand at all fibre contents in OMC-MDD and saturated states. This can be attributed to higher volumetric proportion of 6mm fibre and due to associated higher void space.

The compression indices of fibre reinforced sand at 1.5% fibre content by weight) for 6mm and 12mm length fibre are observed to increase by 3.05 and 2.3 folds compared to Cc value of unreinforced sand under study. However, the values of fiber reinforced fine sand at 1.5% fibre content (0.113 and 0.085 for 6mm and 12mm length fibres respectively) are much less than the compression index of low compressible soils. Hence, the values are insignificant in terms of inducing excessive settlements when used as fill or backfill materials in civil engineering constructions.

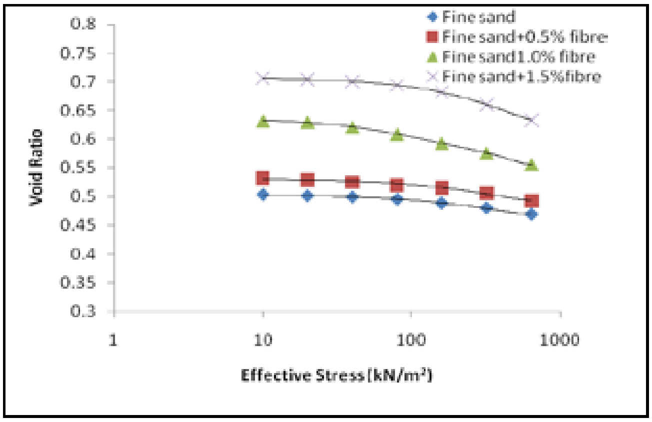

Fig. 1 : Void ratio-effective stress plots of unreinforced and 6mm length fibre reinforced fine sand in soaked condition

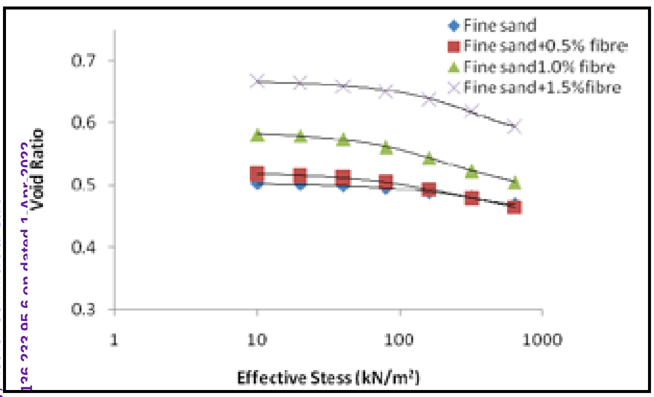

Fig. 2 : Void ratio-effective stress plots of unreinforced and 12 mm length fibre reinforced fine sand in soaked condition

5. CONCLUSIONS

The following conclusions are drawn from the experimental studies carried out on polypropylene fibre reinforced fine sand.

- 12mm length fibre reinforced fine sand has less Compressibility at fibre contents of 1.0% and 1.5%.
- Compressibility of fine sand under study increased by 3.05 and 2.3 times with addition of 6mm and 12mm length polypropylene fibres respectively at 1.5% fibre content.
- Compressibility of fibre reinforced sand up to 1.5% fibre content under study is less than compressibility of low compressible soils.

Hence, polypropylene fibre reinforced fine sand may be considered as fill / back fill material with fibre contents up to 1.5% by weight as it does not cause excessive compression under loads due to lesser compressibility values.

ACKNOWLEDGEMENTS

The author acknowledges the sincere and dedicated efforts put in by Ms. M.R. Aparna, Post Graduate student, Geotechnical Engineering Division, Department of Civil Engineering, Andhra University, Visakhapatnam in conducting laboratory consolidation tests.

REFERENCES

1. Greeshma, P.G. and Mariamma Joseph (2011). Rice straw reinforcement for Improvement in Kuttanad clay", Proceedings of Indian Geotechnical Conference, Kochi, pp. 449-452.
2. Hesham M. Eldesouky, Mohamed M. Moury and Mohamed M Mansour (2016). Fibre reinforced sand strength and dilation characteristics, Ain Shams Eengineering Journal, 7(2), 517-526.
3. IS 1498 (1970). Indian Standard – Classification and Identification of soils for general engineering purpose, Bureau of Indian Standards, New Delhi.
4. IS 2720 - Part 8 (1983). Methods of test for soils – Determination of water content – dry density relation using heavy compaction, Bureau of Indian Standards, New Delhi.
5. IS 2720- Part 15 (1965). Methods of test for soils - Compressibility of soils, Bureau of Indian Standards, New Delhi.
6. Kumar, S. and Tabor, E. (2003). Strength characteristics of silty clay reinforced with randomly oriented nylon fibres", Electronic Journal of Geotechnical Engineering (EJGE), Vol 8(B), 1-11.
7. Satyanarayana Reddy, C.N.V. and Sireesha, G. (2014). Effect of randomly distributed synthetic fibre in fine sand and fly ash, Indian Journal of Geosynthetics and Ground Improvement, CBIP, 3(1),12-17.
8. Sireesha, G and Satyanarayana Reddy, C.N.V. (2018). Effect of randomly oriented synthetic fibre on clay of high compressibility, Indian Journal of Geosynthetics and Ground Improvement, 7(1), 3-10.
9. Venkatappa Rao, G., Dutta, R.K. and Ujwala, D. (2005). Strength characteristics of sand reinforced with coir fibres and coir geotextiles, Electronic Journal of Geotechnical Engineering, USA, Vol.10/B
10. Viswanadham, B.V.S, Phani Kumar, B.R and Mukherjee, R.V (2009). Swelling behavior of geofibre reinforced expansive soil, Geotextiles and Geomembranes, 27(1), 73-76.
11. Yetimoglu,T. and Salbas, O.(2003). A study on shear strength of sands reinforced with randomly distributed discrete fibres, Geotextiles and Geomembranes, 2(2), 103-110.

APPLICATION OF NANOFIBER TO ENHANCE THE ANTI-CLOGGING PROPERTY OF PREFABRICATED VERTICAL DRAINAGE (PVD)

Prasanta K. Panda[1] and Archana Gangwar[1]

ABSTRACT

Prefabricated vertical drains (PVD) are one kind of geotextile filter for the consolidation of soft soil before the building of structure. This consists of a plastic core with grooves on both sides along its length, surrounded by a geotextile filter. The formed groove acts as water channel even at large lateral pressure whereas, surrounded geotextile filter maintain the hydraulic capacity of the grooves preventing clogging by soil intrusion. When the pore size of surrounding filter is larger than the fine soil particle, internal water flow paths of PVD gets clogged by fine soil particles under lateral soil pressure. Intrusion of many fines could reduce the PVD discharge capacity and increase the filter resistance. This filter jacket with appropriate pore size can be used to prevent the clogging and maintain the hydraulic capacity of the grooves. To achieve the appropriate small pore size, thin nanofibrous membrane has been deposited on spun bond nonwoven filter jacket membrane using needle less electrospinning system. During electro spinning, parameters were optimized to get uniform bead less nanofiber layer with required diameter. Further, thickness of nanofiber mat was standardized to keep the pore size less than the soil particle size present in the marshy land soil. Anti-clogging property and water permeability of the membrane with nanofiber layer were investigated after continuous use for a long time in presence of soil. Results showed that use of nanofiber membrane rather than only nonwoven membrane, significantly improves anti-clogging property and maintain constant water flow. The intrusion of soil particles in the membrane pores has been observed by Scanning Electron Microscope (SEM) after use.

Key words *: Prevertical drainage, fine soils, nanofiber, anticlogging, water permeability*

1. INTRODUCTION

Geotextiles are permeable textile materials which are being used with sand, soil and rock in various areas of geotechnical structures such as roads, river and sea bank protection, canal lining, landfills, airport, railways etc. Based on the end use applications, they may be woven, non-woven or knitted as per the requirement. Among the various functions of geotextiles, filtration is an important function to separate water from soil. This is because geotextiles are porous to allow the liquid flow across their manufactured plane and also within their thickness [1].

Prefabricated vertical drains (PVD) are one kind of geo-filters for the consolidation of soil before the building of structure. This consist of a plastic core with formed grooves on both sides along its length surrounded by a filter membrane. The formed grooves act as channel and allow water to flow even at large lateral pressure whereas, surrounded membrane maintains the water flow to the grooves preventing clogging by soil intrusion [2-5].

The pressure drop across the filter media can be expressed as $Dp = \beta\eta V/A$ where Dp is the pressure drop, β is the resistance of filter medium, η is the viscosity of the fluid and V/A is flow rate per unit area. Resistance of filter medium β = mass per unit area of the medium [6]. This relation shows that, increase in resistance of the membrane causes increase in pressure drop. Other than the mass per unit area of the filter media, clogging of pores also cause the hike in resistance. At certain environment for example marshy land soil, particles are smaller than the filter pore, under lateral soil pressure the internal water flow paths of PVD gets clogged by intrusion of those fine soil particles and increase the filter resistance [7, 8]. This phenomenon reduces the water flow and affects the consolidation process. This can be solved by making pores smaller in size to prevent clogging and larger in numbers to maintain the hydraulic capacity of the grooves. Smaller pore size with increase in number of pores per unit volume is possible by deposition of nanofiber layer over the existing nonwoven media.

In this study, Nylon 6 nanofiber has been deposited on the surface of the spun bonded polypropylene jacket to minimize the pore size and improve the anti-clogging property of that geotextile. The modified PVD with nanofiber layer has been compared with conventional PVD with respect to the clogging and filtration efficiency.

1. The Bombay Textile Research Association, LBS Marg, Ghatkopar (W), Mumbai

2. EXPERIMENTAL

2.1 Materials

Fiber grade Nylon 6 of MFI 35 was purchased from J. K. Polymers Surat (India). Spunbonded nonwoven Polypropylene fabric was supplied from Techfab (India) Industries Ltd, Daman (U.T). Acetic acid (MW 60.05 g/mol) and formic acid (MW 46.05 g/mol) was procured from Merck life science Pvt Ltd., Mumbai (India). All these chemicals were used as it is without any further purification.

2.2 Methods

The measured amount of acetic acid and formic acid in required ratio were taken in a conical flask and stirred using magnetic stirrer. Then polymer was added slowly during stirring and kept for 2h at 70˚C. The nanofiber was spun using needleless electrospinning machine NS IS500 U from ELMARCO (Czech Republic) with wire electrode. Electrospinning parameters such as concentration of polymer, positive electrode voltage, negative electrode voltage, distance between the electrode and relative humidity were standardized to get fiber with required diameter. Morphology of Nylon 6 nanofibers was observed by Scanning Electron Microscope (SEM) JSM 5400 from JEOL after gold coating. Quantachrome's 3G porometer operating under windows ® the 3G win software was used to analyze the pore size of nanofiber layer. Water permeability in presence of soil was measured by using falling water head test instrument indigenously made in our laboratory which is shown in Fig 1. In this falling water head tester, water was flown through the sample from a constant water head and time was recorded after 5cm falling of water head. In order to maintain the water head pressure constant, reading was taken after 5cm from the initial point every time.

Fig. 1 : Falling head water permeability tester

3. RESULTS AND DISCUSSION

3.1 Standardization of electrospinning parameters

Effect of different electrospinning parameters such as concentration of polymer, applied voltage, relative humidity %, and distance between electrodes was standardized based on the fiber uniformity and pore size. The value of one parameter was varied within a certain range keeping all other mentioned parameters fixed in a given set of experiment. After the experimentation, standardized values for polymer concentration, applied voltage, relative humidity % and distance between electrodes were found to be 13wt%, 35kV, 45% and 130mm respectively. The nanofiber spun at standardized parameter was uniform in diameter and free form beads. The SEM image of nanofiber at standardized parameters is given in Figure 2 and cross section of the PVD jacket with nanofiber layer is given in Figure 3.

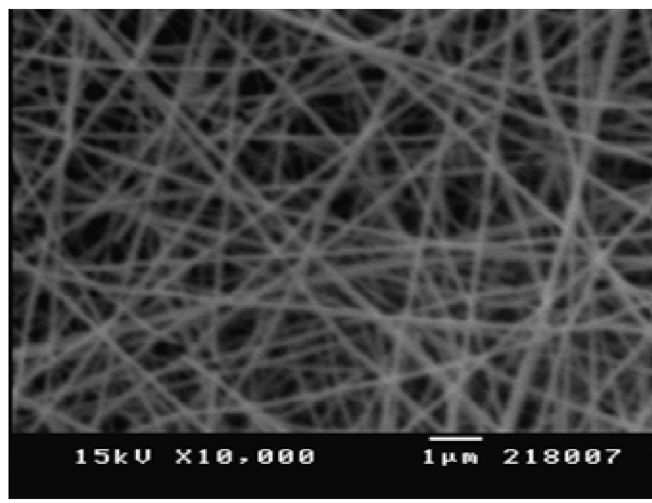

Fig. 2 : SEM image of Nylon 6 nanofiber at standardized parameters

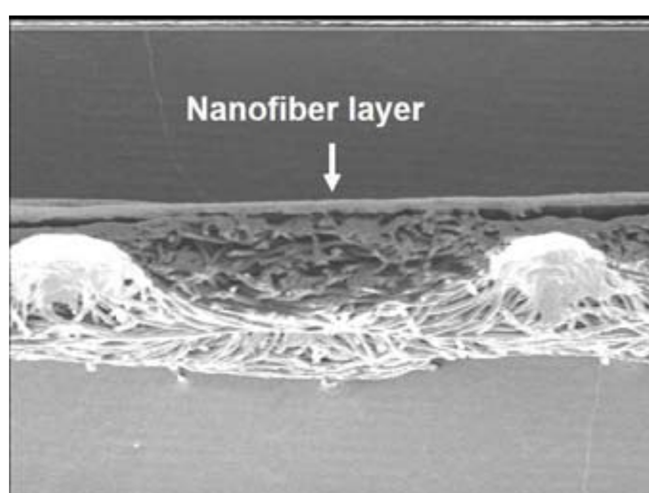

Fig. 3 : Cross section of the PVD filter jacket

3.2 Soil particle size analysis

Marshy land soil contains very tiny soil particles therefore the particle size analysis is very essential to standardize the pore size of nanofiber mat. The collected marshy land soil was taken for particle size analysis. Particle size distribution of the soil is given in Figure 4. Approximate size of the 10% particle was within 2.17 µm and size of the 90% particle was within 92.95 µm in the simulated soil sample. Based on the particle size present in soil, pore size of the nanofiber layer was optimized below 2µm by changing the deposition time of nanofiber layer.

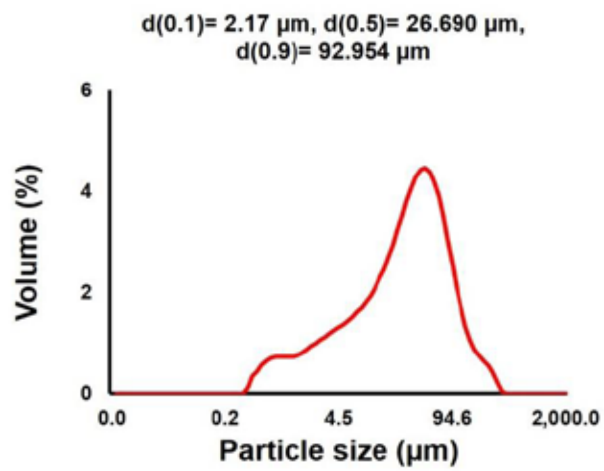

Fig. 4 : Particle size distribution of marshy land soil

3.3 Effect of deposition time on pore size and water permeability

Thickness of the nanofiber mat is inversely proportional to the water permeability so at standardized spinning parameters, thickness of nanofiber mat was standardized by varying the deposition time from 0.5 min to 5 min. Significant increase in pore size and water permeability was found at 1 and 0.5 minute of deposition. As decrease in pore size causes increase in filtration resistance and increase in pore size is not favorable to enhance the anti-clogging property of PVD, 2 min of deposition time was kept fixed for the further investigation. The average pore size in 2 min deposited nanofiber mat was found to be close to 0.558µm.

3.4 Water permeability of the nanofiber deposited media in presence of soil

The water permeability of the existing media and nanofiber deposited media was evaluated by falling water head tester in presence of soil particles. Evaluation was done by changing the soil concentration 1 to 4% on the weight of water. At 1 and 2% soil more water flow was observed in existing media compared to nanofiber deposited media but reverse of this trend was observed at 4% concentration of soil. The water flow was found similar for both the media at 3% soil, so this concentration was taken to study the performance of nanofiber deposited media in long term use. In this experiment both the media was kept continuously in presence of soil for long time and time taken for water head fall to 5cm was recorded continuously. The plot of water head fall time per centimeter corresponding to duration is given in Fig 5. Initially, time taken by water head to fall 1 cm was less in existing nonwoven media compared to nanofiber media but after some hour, it increased and crossed the time taken through the nanofiber deposited media. This was because of low filtration resistance of existing non-woven media which was increasing after some hours by intrusion of fine soil particles and clogging of pores. This phenomenon was not observed in the case of nanofiber deposited media.

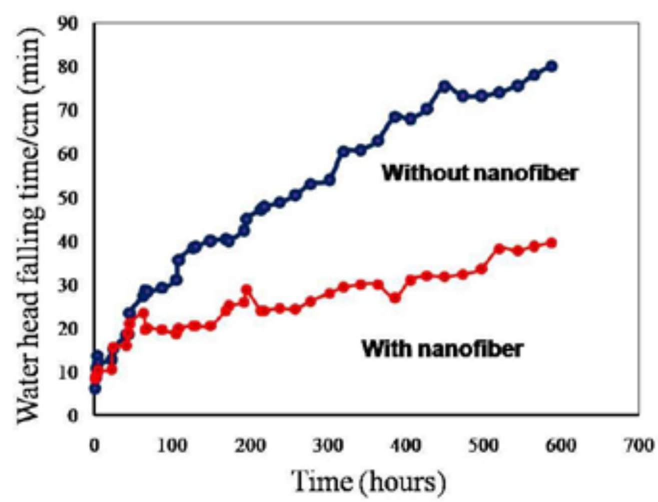

Fig. 5 : Water head falling time after continuous use in presence of soil

3.5 SEM analysis of used sample

The clogging behavior of filter media after use was investigated by the scanning electron microscope (SEM). Both the samples were collected from the tester after use and taken for the analysis. Cross sectional image of both the samples are shown in Fig 6(a) and (b). Intrusion of fine soil particles into the pores was seen in conventional microfiberous media but it was not seen in case of nanofiber deposited media. The pores of the microfiber media were found clean due to the presence of nanofiber layer on it.

4. CONCLUSION

The electro spinning parameters were standardized for Nylon 6 in the needle less electrospinning machine with wire electrodes. Deposition time was standardized to

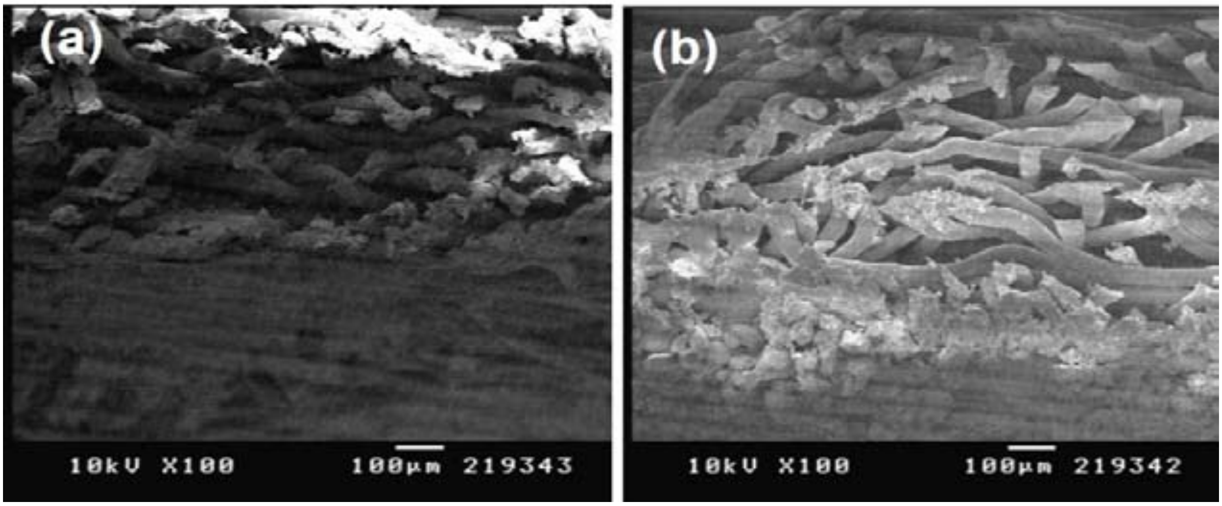

Fig. 6 : Cross sectional view of used nonwoven media (a) without nanofiber (b) with nanofiber

obtain the required pore size in the nanofiber mat. The clogging behavior and water permeability of the PVD substrate with nanofiber mat was investigated for long time in presence of soil. Gradually decrease in water permeability was observed in existing nonwoven media compared to nanofiber deposited media. This increase in time was due to clogging of pores of nonwoven media by intrusion of fine soil particles. Clogging of the pores was confirmed from the scanning electron micrograph. Deposition of a thin nanofiber layer on the existing nonwoven filter media can be helpful to maintain the water flow through the channel and reduce the consolidation time before the construction.

REFERENCES

1. Handbook of Geotextiles, The Bombay Textile Research Association, ISBN 978-81-7674-132-3, 3- 6, 2012.
2. Vertical Drains and Smear Effects: A Brief Review, A. Dey, Geosymposium, 333-335, 2008.
3. B. Indraratna, C. Rujikiatkamjorn, V. Wijeyakulasuriya, G. McIntosh,R. Kelly, Research online, http://ro.uow.edu.au/engpapers/334 , 2007.
4. B. Indraratna, C. Rujikiatkamjorn, V. Wijeyakulasuriya, G. McIntosh,R. Kelly, Research online,227-246, 2010.
5. S. D. Chaugule, J.N.Gulvi, M. B. Mulik, A. S. Yelve, Miss. Pritee, Mistry International Journal on Recent and Innovation Trends in Computing and Communication, 4(4), 286-287,2016.
6. H.J. Choi, M. Kumita, S. Hayashi, H. Yussa, M. Kamiyama, T. Seto, C. J. Tsai, Y. Otani, Aerosol and Air Quality Research, 17, 1052-1062, 2017.
7. N. Miura, Y. Park, M. R. Madhav, Journal of the Japanese Society of Civil Engineers, 483/III-25, 31-40, 1993.
8. G. Mesri, D.O.K Lo, T.W. Feng, ASCE proceedings of the Prediction Symposium during the Settlement, 94ASCE Conference at Texas A&M University, College Station, Texas, USA, 1994.